



HAL
open science

Optical Remote Sensing in Urban Environments

Xavier Briottet, Nesrine Chehata, Rosa Oltra-Carrio, Arnaud Le Bris,
Christiane Weber

► **To cite this version:**

Xavier Briottet, Nesrine Chehata, Rosa Oltra-Carrio, Arnaud Le Bris, Christiane Weber. Optical Remote Sensing in Urban Environments. Land Surface Remote Sensing in Urban and Coastal Areas, 2016, 10.1016/B978-1-78548-160-4.50001-7 . hal-02292949

HAL Id: hal-02292949

<https://hal.science/hal-02292949v1>

Submitted on 12 Dec 2024

HAL is a multi-disciplinary open access archive for the deposit and dissemination of scientific research documents, whether they are published or not. The documents may come from teaching and research institutions in France or abroad, or from public or private research centers.

L'archive ouverte pluridisciplinaire **HAL**, est destinée au dépôt et à la diffusion de documents scientifiques de niveau recherche, publiés ou non, émanant des établissements d'enseignement et de recherche français ou étrangers, des laboratoires publics ou privés.



Distributed under a Creative Commons Attribution - NonCommercial 4.0 International License

Optical Remote Sensing in Urban Environments

Xavier BRIOTTET, Nesrine CHEHATA, Rosa OLTRA-CARRIO,
Arnaud LE BRIS and Christiane WEBER.

1.1. Introduction

1.1.1. *The urban system*

Cities today face a variety of issues: attractiveness and economic development, living conditions and urban redevelopment, the quality of life of citizens and the environmental conditions of the urban system as a whole.

These challenges reflect the situations in urban territories where the economic development and population growth required for stabilizing the urban system come into conflict with the promotion of esthetic urban improvements appropriate for social cohesion and ensuring the safety of users while guaranteeing a reduction of the environmental impact caused by urban spread [WGI 14, WEB 15, MAC 07, WIL 11]. The process of urbanization, which has significantly transformed our countryside over the last hundred years, was the most important factor of the 20th Century and saw the urban population surpass the rural population in the majority of Western countries.

The process of urbanization can be defined as “particular forms and structures of space being occupied by the population [RHE 14]” – in other

words the transformation of space (natural, agricultural, forest, etc.) through human activity. A recurrent problem is the objective demarcation of the urban system which is partly artificial and difficult to transpose from one case to another (conurbation, administrative boundaries, etc.). The determinants can vary in time and space (from one country to another¹). In fact, identifying the place of study can sometimes get in the way of properly understanding the dynamics of urban growth and expansion, because like any other system, it is not exempt from external factors which influence its internal dynamics. For instance, environmentally evaluating the quality of the water supply can be carried out at various locations in the urban system: where the water is extracted from, where it leaves the urban system and in the city center. The quality of the supply can only be determined based on sections that have been artificially developed.

What makes the urban space so complex is that it only exists insofar as it is “built, worked and used through social ties” [CAS 72]. It can be thought of as a construction where the organization and the structure impact upon urban society but also as one element of a much wider ecosystem on which it depends and/or which it influences. This system incorporates political, economic, social and, increasingly, environmental dimensions and we therefore see it as a complex and heterogeneous ecosystem whose social, technical and natural components must be studied in order to understand the way in which it functions [MAT 06]. Taking these dimensions into account is necessary for urban studies, whether this is in terms of evaluating environments, modeling dynamics or outlining evolution scenarios.

Over the past few years, the focus has been on gaining a better understanding of how the urban ecosystem works. This has taken place under different investigations:

- a study focusing on the social, economic and spatial aspects of the urban system in order to consider the environmental aspect;
- another study which focuses more on the interactions between the urban ecosystem as a whole and the natural systems on which it depends.

This study examines both the fluctuations (energy resources, food, raw

¹ The space considered here rarely corresponds to the administrative body as defined by the National Institute of Statistics and Economic Studies (INSEE) but more generally to the morphological urban zone taking into account the expansion of built-up zones built in addition to the employment area.

materials, etc.) and the state of these systems (the state of biodiversity, for example).

Both studies introduce different but compatible problems; for example, the quality of living conditions will be analyzed in the first study by studying the behavior and aspirations of citizens related to the presence or absence of amenities; the second study will focus on disparities in areas featuring particular environmental phenomena (pollution, heat islands, presence of vegetation, etc.). Based on the problems that have been explored, it is necessary to establish a comprehensive framework for spatial and temporal analysis. This framework is essential for detecting, characterizing and identifying a given phenomenon [SAI 06]. It makes it possible to consider the state and dynamic of the urban ecosystem, as well as how its different elements interact with each other. The trio space*time*function [PEU 95] summarizes the complexity of these approaches:

- Space outlines the states of the urban ecosystem. These can be determined according to the general characteristics present, such as buildings, population and employment. This space is characterized through spatial, social and even environmental attributes at a number of levels that are often intertwined.

- Depending on the temporal scale that is chosen, urban dynamics can give us an indication of, for example, changes in land use (LU). These are made available through evolution processes that can sometimes be highlighted by the causes of change. Thus, urban wasteland constitutes a stage in the modification of soil usage (green zone to construction zone) and of a function (a strip of garden to an office block). Increasing demand for urban housing can lead to construction dynamics and increased housing stock which in turn can lead to a rise in urban growth.

- How the urban ecosystem interacts with the natural systems on which it is reliant depends on a number of factors: for instance, the characterization and the use of surface water in the city, urban climate zones [STE 06] or the part played by vegetation in a city's energy patterns.

Thus, new studies have been undertaken and knowledge of a territory as well as how to monitor it is increasingly important. As a result, there is an increasingly pressing need to collect, assimilate and analyze high-quality geographical data which can be put to a variety of uses.

In 2010, Sebari and Morin [SEB 10] demonstrated how satellite imaging could be used for urban studies (*Measuring the evolution of the urban environment, Mapping the LU, Urban planning, Revised cartography or Updated automatic cartography*) following on from the challenges outlined by Donnay *et al.* [DON 00]. Taking these environmental challenges into account has altered the way in which information is gathered by introducing the need to identify the natural components of the urban matrix² and how they interact with the population and activity in a way that is both prospective and retrospective.

Thanks to the acuteness of the information obtained, satellite imaging makes it possible to take into account policy choices which are environmental (protecting habitats, improving green spaces and waste ground), patrimonial or urbanistic (property management and protecting sensitive zones) or pertaining to landscape (reorganizing riverbanks, minimizing the break-up of habitats and improving focus areas). Satellite imaging can therefore be thought of as a medium for (re)presentation, a tool for consultation or even for cooperation. The images provided are used at different stages of the process: detection and observation, how results affect decision making, evaluating action taken and monitoring this action for future reference.

1.1.2. *The urban environment*

The urban environment is a heterogeneous mineral environment, made up of buildings that vary in terms of compactness and morphology³. Transport networks, waterways and green spaces intertwine in the built matrix and this leads to ruptures in the urban landscape. Seen from above, these landscapes

2 The term *urban matrix* refers to the set of components which make up a system (buildings and infrastructure, vegetation, water surfaces, bare earth or waste ground). It is possible to distinguish between the gray matrix (buildings and infrastructure), the natural matrix (vegetation and water) and the brown matrix (soil and waste ground).

3 *Urban morphology* is the study of urban shapes. Urban morphology aims to study the urban make-up beyond a simple analysis of the architecture of buildings and to identify underlying patterns and structures. Urban morphology studies a city's shapes and characteristics (its roads, its plots of land, how areas are divided, density and functions) and the main factors behind it: topography, history, cultural influence, economics, town planning as well as the technological or even the energy context. It is based on different levels of the urban area: buildings, blocks, the urban fabric, the city and its surroundings.

can normally be determined by groups of buildings which appear similar at first sight, but which vary according to their distance from the center(s) by general morphology, the layout of neighborhoods, the space between buildings, how buildings are grouped around a more significant building such as a church or a theater or a square, or even along an avenue, the presence of other ruptures (roads, railway lines and canals) and the presence of vegetation within a built-up area and/or in parks and at the roadside. Depending on their size, their shape or the material used for roofing, buildings can disturb the impression of uniformity. Various studies have successfully defined categories for LU following criteria based on the density of the area, how far it is from the city center and the minimal mapping unit. Within the framework of the CORINE Land Cover (CLC) program, efforts were made to standardize the different categories of LU on a Europe-wide level. From this point onwards, the typology put forward has been expanded and adapted, notably for urban spaces where the minimal zones for representation with CLC (25 ha) are not consistent with the urban scale (1/5000° to 1/20000°).

On this scale, the characteristics of urban environments are as follows:

- areas that are mineral or not and distances between locations (and therefore the density);
- the volume and spatial arrangement of areas;
- the environment's components: built matrix and networks, natural matrix (depending on various strata and water surfaces);
- interior and continuous break lines: coastline, lakes, rivers, road and rail networks, walls or empty lots;
- gradients: from the center toward the periphery. Given that city limits are difficult to identify, the interactions of the city and its surrounding area makes readability complicated;
- materials used to cover mineral surfaces.

The Urban Atlas⁴ program put forward by the European Environment Agency (EEA) proposes covering all towns in Europe with a population greater than 50,000 where the focus will be on functional urban areas

⁴ <http://land.copernicus.eu/local/urban-atlas>.

(functional division where the objective is statistical) defined by ESPON (2006)⁵. The characteristics of the different types of LU (Table 1.1) pick up the large lines above by using more specifically urban density and the distance between a continuous or discontinuous building, and one that is isolated. Artificially created surfaces can be obtained using the Fast Track Laser European Environment Agency (EEA). This product uses several databases as well as satellite data with a resolution of 2.5 m (initial or a fused with the panchromatic channel) ranging from the visible to near-infrared. This is one of the services that is linked to the GMES/Copernicus program⁶.

Type of surface	Object	Shape and organization of the objects (among themselves and in relation to their environment)
Artificial areas	Urban fabric	Continuous urban fabric Discontinuous urban fabric (dense, average and less dense) Isolated structure
	Commercial, industrial, public, military and private units	Commercial, industrial, public, military, transport and private units Roads, rail networks and related surfaces
	Ferry ports	
	Airports	
	Mines, building sites, waste disposal sites	Mineral extraction and waste disposal sites Building sites Wasteland areas
	Green spaces	
Non-agricultural green spaces	Agricultural or semi-natural zones, wetlands	
Forest		
Water surfaces		

Table 1.1. Characteristics of different types of land cover and land use (Urban Atlas, 2012)

⁵ <http://www.espon.eu/main/>.

⁶ http://www.esa.int/Our_Activities/Observing_the_Earth/Copernicus/Overview.

In 2001 Puissant and Weber [PUI 01] were able to establish a way of naming urban objects that can be used for describing the urban matrix based on SPOT images (Table 1.2). In certain cases, the general organization of the built matrix also makes it possible to determine some of the functions of the environment: the presence of air or sea traffic, important road and rail networks, peripheral areas, etc.

Type of surface	Object	Shape and organization of the objects (among themselves and in relation to their environment)
Urban vegetation	Trees	Single trees Grove (clump of trees) Forest Line of trees
	Grass or shrub	Field (park or garden depending on the surrounding area or the type of sports field according to its shape)
Built-up areas	Building	Continuous - dense urban layout (most often facing the road) Discontinuous – large buildings Residential (depending on the size of a building and its surroundings) Isolated
Network	Road	Motorway or four-lane (and more) roads Dual carriageway
	Rail network	Railway lines Rail depot
Industrial zones, airports/sea ports, service	Buildings and infrastructure	Building layout, carparks, proximity to networks
Interstitial mineral areas	Parking Place Building area	
Water pond	Rivers, canals, ponds, lakes etc.	Shallow water networks

Table 1.2. Typology of useful urban objects (taken from [PUI 01])

Satellite images can thus be thought of as one aspect of a wider information network that is used for studying the urban ecosystem. Changes caused by the digital boom have radically changed the situation since the end of the 20th Century. The potential for benefiting from localization, description and valorization in 2D or 3D via paying or free networks has led

to the spread of digital media and their use as a spatial reference. The contribution of various sources of information makes it possible to reuse satellite images alongside existing databases for a given area. Since then, satellite imaging has been one of a number of elements used (national or international databases, shared collective data, online information, of variable internal and external quality). An additional advantage of satellite data is the stability of the data provided and the capacity to obtain different data modulated by the number of sensors, the spectral range or the spatial resolution. Through the changing ways in which the Earth is observed, satellite imaging meets a variety of demands (observation, measurement, modeling, representation and application) while continuing to reframe the debate over how we study the environment. The current range is expanding in order to meet the latest challenges concerning the anthropization of areas by making technical improvements which will enable better results.

1.1.3. The main characteristics of the urban environment: geometric, spectral and temporal

The urban environment is characterized by the heterogeneity of its shapes, materials and density. Furthermore, a city is made up of large buildings and their shapes create shadows which increase its complexity on the radiative understanding.

1.1.3.1. Geometric characteristics of urban objects

The geometric diversity of urban objects is caused by several factors such as density, the age of the city or its latitude. Since the 1980s [CLA 80, WEL 82], determining the optimal spatial resolution in order to identify urban elements has been a key issue for the new generation of sensors. While in North America a resolution of between 20 and 30 m is considered acceptable, a resolution of between 20 and 10 m, or even metric resolution has become the necessary threshold for the use of satellite imaging in town planning. Small [SMA 03] used IKONOS images with a spatial resolution of 1 m in order to determine the average size of urban objects across 14 cities worldwide and was able to show that it is somewhere between 10 and 20 m. Resolution of 5 m or below is considered necessary for the accurate representation of urban objects for the following applications: buildings, roads and their aging process [HER 05], the spread of urban vegetation [WEN 07, JEN 12] and land planning [PUI 03, PUI 04, WAN 07a].

Following a study of useful urban objects in Strasbourg (France), Puissant and Weber [PUI 01] were able to draw up a table of optimal resolutions using simulated SPOT images (XS and P) with resolutions ranging from 5 to 1.36 m (Table 1.3). The results indicate that a fine resolution of 1.36 m is necessary in order to identify “dense urban” buildings, while a resolution between 2.5 and 5 m is sufficient for identifying “large group” buildings; a resolution of 2.5 m is sufficient for identifying vegetation and roads.

Reference objects	10 m	5 m	2.5 m	1.36 m
<i>Trees</i>	X	X	X	X
<i>Fields</i>	X	X	X	X
<i>Interstitial green spaces</i>		X	X	X
<i>Dense urban</i>	X	X	X	X
<i>Large groups</i>	X	X	X	X
<i>Roads</i>	X	X	X	X
<i>Railway lines</i>			X	X
<i>Interstitial mineral areas</i>	X	X	X	X
<i>Water</i>	X	X	X	X
<i>Shadow</i>	X	X	X	X
<i>Rate of well classified pixels</i>	8 classes 85 %	9 classes 89 %	10 classes 86 %	10 classes 80 %

Table 1.3. Urban typology and spatial resolution for the city of Strasbourg [PUI 01]

1.1.3.2. Spectral characteristics

A city can be said to be made up of three types of areas: mineral areas (buildings, infrastructure and bare soil), vegetation and water. The spectral signature of these areas depends on their chemical composition, the acquisition time (day/night) and the surrounding environment. Spectral signature is influenced by several parameters which play a more significant role depending on the given spectral range: reflectance, emissivity and surface temperature.

These optical parameters (detailed in section 1.1.4) are characteristics of the chemical composition (spectral signature), the surface state (spectral

and/or directional signature) and the time of measurement (directional signature) for a given material.

1.1.3.3. *Temporal characteristics*

The urban system offers a range of dynamics depending on the components being considered. Vegetation follows the seasonal vegetative cycle (soil, sunlight and weather conditions) while being strongly influenced by factors such as the shapes of buildings and the specific ecological conditions of a given environment.

The development of buildings covers various dynamics:

- the growth of built-up areas (residential, industrial and the different types of network) outside of the urban matrix through urban sprawl: the standardization of the production process has considerably shortened construction time. However, observing the creation of a built-up area is only possible by observing the change in LU. Of course, this is also connected to the size and localization of the modified surface. This is why development seems fairly slow, because on the one hand only groups of buildings can generally be observed while on the other hand, such changes are taking place in pre-existing construction units;

- the filling-in of built-up areas within the urban matrix: the construction of a new building where an old one previously stood or the use of waste ground tends to be difficult to observe without close monitoring;

- urban materials have their own intrinsic dynamics depending on the composition of the used material (aging or dirty tiles) as well as extrinsic dynamics relating to the use of new materials, including, for example, materials with a higher capacity for retaining heat.

We can see therefore that the system's heterogeneity is an essential element in the temporal dimension of both the urban matrix and the dynamics related to its components.

1.1.4. *Optical properties of urban materials*

1.1.4.1. *Spectral signatures*

The range of different urban materials of various chemical compositions leads to a wide variety of spectral signature in the optical domain. Several

authors have carried out studies in order to obtain spectra of urban materials in the reflective field [BEN 01, HER 04, SOB 12a] as well as in the optical field [BRI 06]. By way of an illustration, Figure 1.1 and Figure 1.2 shows the spectral signature of urban materials in the range (0.4–2.5 μm) (and [3.0–14.0 μm]) respectively. In the range (0.4–2.5 μm), tile roofs and bricks have similar signatures. It is only possible to distinguish between these two types of surfaces using the spectral signature through the use of a spectral imaging device.

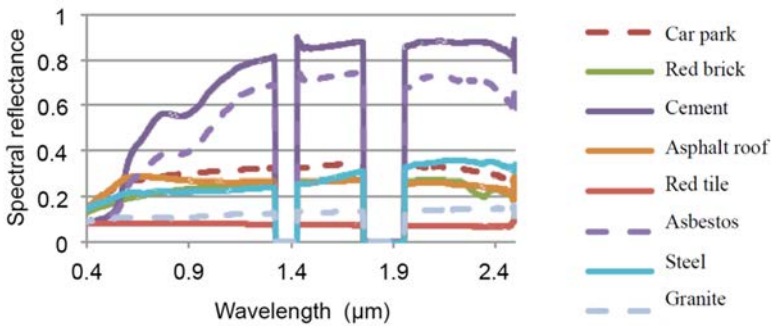


Figure 1.1. Average spectral reflectance of urban materials measured in Madrid in the range [0.4–2.5 μm] [SOB 12a]. The absence of measurements around 1,4 and 1,9 nm corresponds to high water absorption bands in the atmosphere. For a color version of this figure, see www.iste.co.uk/baghdadi/5.zip

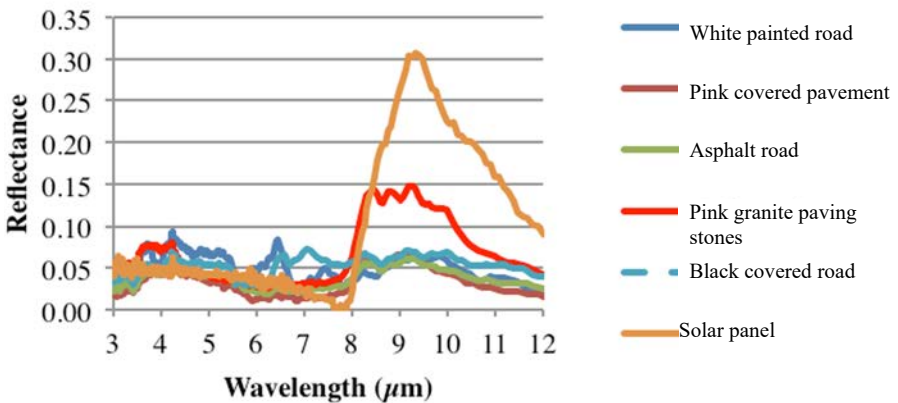


Figure 1.2. Average spectral reflectance of urban materials in the range [3.0–14.0 μm] [BRI 06]. For a color version of this figure, see www.iste.co.uk/baghdadi/5.zip

Figure 1.2 shows that surfaces such as roads and pavements covered with asphalt and minerals have a similar spectral behavior due to the dominant presence of hydrocarbon on the surface. There is an increase in reflectance for granite paving stones caused by the presence of the carbonate ion CO_3^{2-} . The presence of silicate in solar panels results in an increase in reflectance around $10 \mu\text{m}$.

The high diversity in spectral signatures is used in hyperspectral imaging in order to distinguish between materials [JEN 12, BEN 01] and to estimate their state [HER 05]. As it is shown, similar spectral signatures can represent different kinds of objects (an asphalt roof and an asphalt road for example), but it is still possible to distinguish between them. This can be done using hyperspectral images combined with data obtained either from an airborne 3D LiDAR, or from a digital surface model (DSM) (detailed in section 1.2.1.2).

1.1.4.2. *Intraclass variability*

However, for the same material, there can be distinct variations in its signature and this leads to a change in the classification or unmixing techniques: this is called intraclass variability. There are several reasons for this variability:

- physical (difference in texture or roughness);
- use (for instance, the signature of asphalt will not have the same signature on a pavement as it will on a road due to different deteriorations);
- definition of classes (for instance, granite can include different colors and different components).

By way of an illustration, Briottet *et al.* [BRI 06] were able to quantify this variability for the city of Toulouse, summarized in Table 1.4 for a sample size of 20 cm. A maximum standard deviation is calculated corresponding to the maximum of standard deviations calculated for each of the different types of intraclass variability. The analyzed classes include different types of asphalt, cement, granite, brick and tile. The strong relative standard deviation (%), found for physical intraclass variability in the range ($3.0\text{--}12.0 \mu\text{m}$), is caused by the diversity of materials included in each class, but also due to the weak level of reflectance (given that the standard deviation is of the same magnitude as the reflectance, the resultant relative standard deviation, defined as the link between the standard deviation and the reflectance, is large).

Type of variability	Maximum standard deviation in the range (0.4-2.5 μm)	Maximum standard deviation in the range (3.0-12.0 μm) (%)
Physical	13	88
Use	30	21
Class definition	50	40

Table 1.4. Maximum standard deviation of the intraclass variability of the reflectance across all classes measured in Toulouse in the optical domain

Table 1.5 shows that the used classification used has a significant impact on variability. The influence of the texture of the material is highly variable depending on the given spectral domain.

Level 1	Level 2: Type of soil	Level 3: Type of material	Level 4: Surface material		Characteristic wavelengths (nm)
Artificial surfaces	Building/roof	Mineral material	Asbestos	Asbestos	580, 800, 2,323, (2,320; 944)
			Asphalt roof	Asphalt roof	1,700, 2,350, 11,300
			Clay roof (red)	Clay roof (red)	520, 670, 870, (iron ion absorption)
			Concrete roof	Concrete roof	A 2,300–2,370 (calcite and dolomite), A 2,170 (argile), 1,413 and 2,323 (portlandite, muscovite)
			Gravel	Gravel	Silicate 2,200, carbonate 2,200, iron oxide 520, 670, 870
			Plate glass window	Plate glass window	R 372, 400 A 2280
		Slate	Slate	R 791, A 940, 2,200, 2,260, 2,340	
		Metallic material	Aluminum	Aluminum	A 840
			Copper	Copper	R 540–650, A 2,240, 2340
			Zinc	Zinc	A (strong) 550 A 1,020

		Polyvinyl chloride	Polyvinyl chloride	Strong absorption of 1,200, 1,700, 2,170, 2,300
		Polyvinyl (PV)	Monocrystalline silicon(Si)	732, 1,100
			Gallium Arsenide (GaAs), Indium Gallium Phosphide (GaInP)	381, 887
			PV	732–1,067 (Optimal transmission window)
	Vegetal material	Green roof	Green roof	R 550, 750, A 450, 680, 980, 1,200, 1,400, 1,900
		Thatched roof	Thatched roof	Cellulose vibration A 2,100, 2,300
		Wooden roof	Wooden roof	Cellulose vibration A 2,100, 2,300
	Waterproof surface	Asphalt	Asphalt	Weak absorption 1,850, 2,315, 2,350
				1,700, 2,350, 11,300
		Cement brick	Cement brick	R 600–700, Iron oxides A1,410, A1,940–1,970, mini reflectance of gray cement 2,310–2,350
Artificial water surface	Swimming pool	Swimming pool	A 1,340–1,480 and 1,770–1,970	
	Garden pond			Garden pond

Table 1.5. Extract of the characteristics of urban materials [ZIN 15] (A: absorption; R: reflectance)

1.1.4.3. Directional variability

With urban materials, there is also a wide variety of directional behaviors [BRI 16] which is due in large part to their roughness. Thus, a smooth surface such as a solar panel or polished granite will show marked specular reflection, while a rough material (such as tiles or rough casting) will have a maximum of reflectance in the backscattering direction.

Examples of directional behavior are given in Figure 1.3 where the directional reflectance of different artificial materials is outlined in polar

representation. Thus, with concrete, asphalt and pink granite, the peak of reflection is in a forward direction. The measured granite has a smooth surface which explains the higher amplitude of the reflection peak. However, asphalt does not display a marked directional signature (Lambertian reflectance).

1.1.4.4. Temporal variability

The materials found in a city undergo natural changes (evolution of vegetation along a year), but they are also chemically damaged (pollution) and through use (changes to the surface). This modifies their spectral signature and can thus be used as an indication on their status. Herold *et al.* [HER 05] were able to estimate the aging and deterioration of roads using ground spectrometric measurements. These modifications are attributed to physical changes (through use) and chemical changes to the road surface.

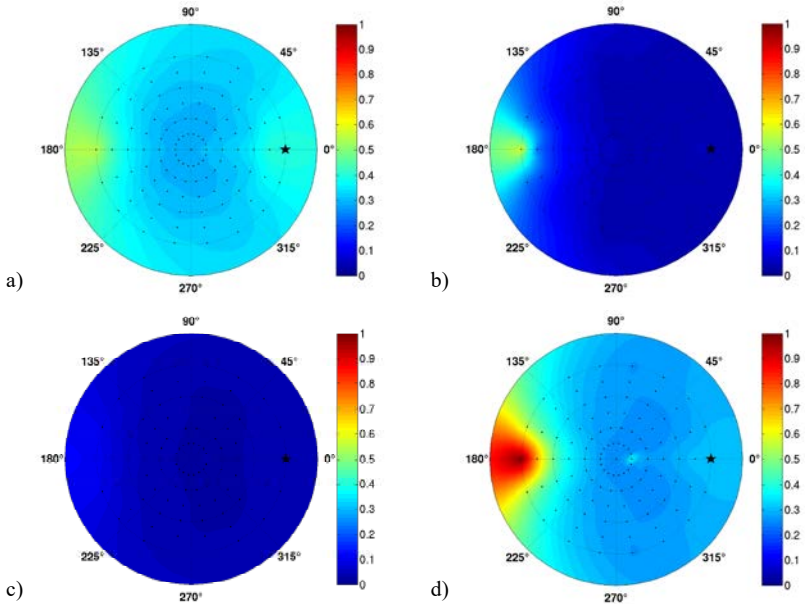


Figure 1.3. Bidirectional reflectance of different urban materials at 550 nm for an incident zenith angle of 60° (size of the sample measured at nadir of 20 cm): a) concrete, b) red asphalt, c) asphalt and d) pink granite. In a polar representation, the length of the radius represents the zenith angle, the angle between this radius and the x axis is the azimuthal angle and the color represents the value of the bidirectional reflectance. The star indicates the position of the light source. For a color version of this figure, see www.iste.co.uk/baghdadi/5.zip

1.1.5. Spectral characteristics

1.1.5.1. Introduction

In remote sensing, the interpretation of the signal acquired over an urban environment is very complex because of its specific structure which causes occultations, shadows, light reflected by facades and the directional effects of the materials present. These processes make it difficult to interpret the signal received and to automatically determine the materials present directly from the signal measured by a sensor. Figure 1.4 illustrates the radiative components present in remote sensing at high spatial resolution⁷ optical imagery, in particular.

- shadows are classified separately (in black in Figure 1.4(a));
- roofs of the same material but with different slopes are classified separately (in blue, green, yellow and cyan in Figure 1.4(b)).

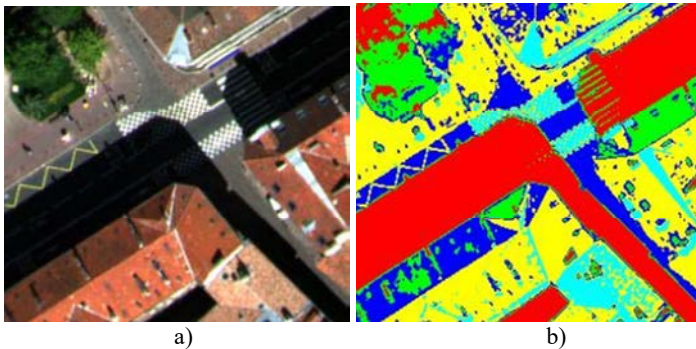


Figure 1.4. a) Colored composition of an image acquired for Toulouse by the multispectral airborne camera PELICAN (spatial resolution of 20 cm) and b) non-supervised classification for the same area (ONERA credit). For a color version of this figure, see www.iste.co.uk/baghdadi/5.zip

A degradation of the spatial resolution (Figure 1.5) leads to a loss of geometric details and several objects can be contained in a single pixel. Furthermore, lower spectral resolution makes it more difficult to discriminate between different materials.

⁷ For decametric spatial resolutions, we will refer to high spatial resolution (HR) and for resolutions between metric and submetric we will refer to very high spatial resolution (VHR).



Figure 1.5. Images of Toulouse at three spatial resolutions of 30, 8 and 2 m generated from data obtained from the airborne multispectral camera PELICAN during the Musarde experiment (ONERA/IGN credit, 2010). For a color version of this figure, see www.iste.co.uk/baghdadi/5.zip

For applications such as the soil mapping [LU 06], the growth of cities or changes in LU [MAD 01, JAT 08], hyperspectral instruments with a spatial resolution of roughly 30 m are used. For this, the baseline information is the spectral reflectance. The advantage of these instruments is that their swath makes it possible to cover vast urban areas. However, the main disadvantage is that the images are made up of a large number of pixels and include a mix of several different materials. Various studies have been carried out in order to evaluate the contribution of hyperspectral imaging compared to multispectral imaging. Platt and Goetz [PLA 04] show that the classification of urban surfaces obtained from images taken by the spectro-imaging device AVIRIS is better than classification with Landsat ETM+ data. A number of authors [LU 06, WU 03] explain the limitations of multi-spectral sensors for characterizing impervious surfaces and discuss the potential of hyperspectral imaging. Cavalli *et al.* [CAV 08] obtain a similar conclusion in their classification works.

Identifying smaller objects (< 5 m) has become possible using panchromatic and multispectral devices such as SPOT 6/7 and Pléiades satellite sensors. However, such a spatial resolution comes at the expense of spectral quality (the number of bands is limited to 3 or 4 in the visible and near infrared spectrum with a typical bandwidth ranging from 60 to 100 nm). These methods rely on the use of features such as the spectral indices, the geometric shapes [DUR 08, ING 07] and the texture [ZHA 09]. These methods will be outlined in section 1.2.1.

The advent of new spatial missions which combine a hyperspectral camera with a spatial resolution of 8 m for the HYPXIM mission [CAR 14], (10 m for the SHALOM mission [BEN 14]) and a panchromatic camera with a spatial resolution of 1.8 m (4 m for SHALOM) will allow for a better understanding of urban environments. Thus, the joint use of images acquired through these two hyperspectral and panchromatic imaging devices makes it possible to generate a fused image with a high spectral resolution and a high spatial resolution. There are different techniques for this type of fusion. For instance, a comparison of eight methods of panchromatic and hyperspectral fusion was proposed in Loncan *et al.* [LON 15]. The best results were obtained with the methods developed by Laben and Brower [LAB 00], Yokoya *et al.* [YOK 12], Wei *et al.* [WEI 15] and Simoes *et al.* [SIM 15].

The use of airborne imaging rounds off the range of spatial technology through its capacity to acquire images simultaneously with a high spatial and spectral resolution. By way of an illustration, the AVIRIS⁸, HYSPEX⁹ or HYMAP¹⁰ cameras, at their nominal altitude, have spatial resolutions between 2 and 4 m, while covering the range 0.4–2.5 μm . We are currently witnessing the arrival of new devices which are sensitive in the thermal infrared spectrum, such as the TELOPS¹¹ systems, or across the whole optical spectrum, such as the Sysiphe system [ROU 15], with compatible spatial resolutions for observing urban environments.

1.1.5.2. *Spectral preprocessing*

The data acquired by these devices are georeferenced images expressed in radiance units. To extract the perturbing effects of the atmosphere, whether spectral or temporal, preliminary preprocessing specific to urban environments is necessary in order to estimate the following parameters: reflectance, emissivity and/or temperature for applications.

The presence of 3D urban structures creates a lot of shadows which deteriorate the effectiveness of processing for applications such as the identification of urban materials [LAC 08, LEB 96], detecting objects [SHI 11], 3D reconstruction [CHE 11] or monitoring traffic [FLE 06]. To improve these results, two steps are necessary: shadows identification and

8 [Aviris.jpl.nasa.gov](http://aviris.jpl.nasa.gov).

9 <http://www.hyspex.no/>.

10 http://hyvista.com/?page_id=440.

11 <http://telops.com/fr>.

atmospheric correction, in order to estimate the optical properties for surfaces at all points of the image, in the sun and in shadow. We are able to justify this step because the different total incident radiation (for example, there is no direct solar radiation in shadow) means that different types of preprocessing will be applied.

Shadows can be characterized in the reflective domain by the following radiative properties:

- the levels of radiance in shadow are weaker than areas illuminated by the sun;
- the radiative effects of the environment caused by multiple reflections can no longer be disregarded in shadow [LAC 08];
- the spectral radiance measured in shadow decreases as the wavelength increases (decrease in the atmospheric diffusion);
- the spectral radiance measured in shadow depends on the spectral reflectance of the material.

Methods of identifying shadows rely on either one or several of these characteristics. For a detailed comparison of existing methods, we would refer the reader to studies carried out by Adeline *et al.* [ADE 13]. The limitations of current methods are due to the difficulty of separating water from shadow and identifying shadows in the vegetation when it is less dense.

Once the shadows have been detected, different methods of atmospheric correction have been developed in order to reduce the impact of perturbing radiative effects in the city–atmosphere system. In an urban environment, radiative exchange is more complicated than with a flat surface (see Chapter of [BAG 16]). Figure 1.6 illustrates the different irradiance E components incident to the surface at point B in shadow and at point C in the sunlight and radiance L components at sensor level. In the shadow, the direct irradiance E_D is absent, the downwelling atmospheric irradiance $E_{atm,d}$ is no longer integrated over the $2.\pi$ sr but instead over the sky solid angle Ω_{sky} delimited by the 3D shape of the buildings, the coupling irradiance E_C is also reduced by the presence of 3D structures. Finally, a new form of irradiance appears, caused by multiple reflections, E_{refl} , due to the 3D environment of the considered point.

The total incident irradiance, E_T is written as:

$$\begin{aligned} \text{in the sunlight: } E_T &= E_D + E_{atm,d} + E_c + E_{refl} \\ \text{in shadow : } E_T &= E_{atm,d} + E_c + E_{refl} \end{aligned} \quad [1.1]$$

Given that the total radiance at the level of the sensor L_T is the sum of the incident radiance s , and supposing Lambertian reflectance, reflectance ρ at ground level is written as:

$$\begin{aligned} \text{in the sunlight: } \rho &= \frac{\pi.(L_T - L_{atm,m} - L_{envi})}{(E_D + E_{atm,d} + E_c + E_{refl})} \\ \text{in shadow : } \rho &= \frac{\pi.(L_T - L_{atm,m} - L_{envi})}{(E_{atm,d} + E_c + E_{refl})} \end{aligned} \quad [1.2]$$

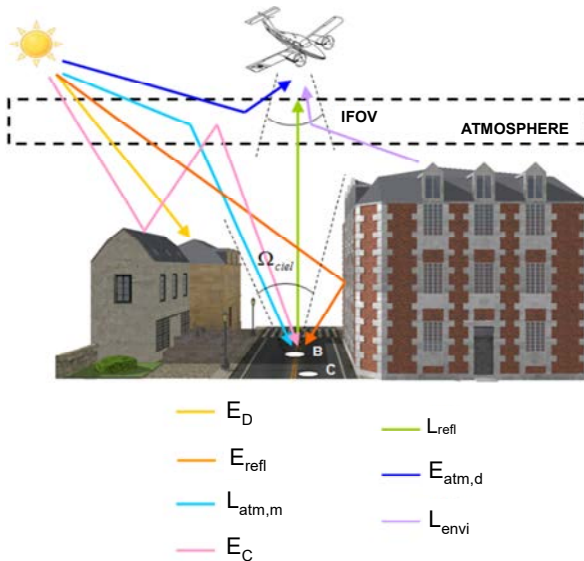


Figure 1.6. Illustrations of the radiative components in E irradiance and L radiance for a surface in the shadow of a building (B) and for a surface in sunlight (C) [ADE 13] For a color version of this figure, see www.iste.co.uk/baghdadi/5.zip

Different methods are then used in order to solve equation [1.2] depending on whether the point is in sunlight or shadow. The first type of method considers the ground as flat and no correction is possible in shadow. The chapter by Briottet in this set of books [BRI 16] provides a description of these methods. Nevertheless, Chen *et al.* [CHE 13] put forward an

alternative by adding empirical geometric correction factors: weighting of the total descending atmospheric irradiance, calculated over the 2π sr by an average of the solid angle of the sky, suppression of the terms L_{envi} , E_C and E_{refl} . This method provides better results but only for the visible domain (VIS). Other more empirical methods aim to equalize the grayscale between the areas in shadow and the areas in sunlight. The disadvantage of such methods is that it is not possible to correct the spectral effects caused by the presence of different radiative terms.

More recent methods (ATCOR-4 [RIC 03], ICARE [LAC 08]) have been developed using a DSM in order to calculate the different terms of equation [1.2] using a radiative transfer code like Modtran. Thus, Lachérade *et al.* [LAC 08] were able to obtain a maximum deviation of 0.04 in reflectance units [BAG 16] for the estimated reflectance in shadow, compared to experimental data. The main sources of error are due to a registration error between the image and the DSM, and the shadow caused by non-opaque trees which allows part of the direct solar irradiance to pass through, which is not taken into account in equation [1.2].

Methods of atmospheric correction in the thermal domain are less sensitive to the environment. Thus, the methods described in the chapter by Briottet [BRI 16] are used. Additional information relating to the urban environment is provided in section 1.3.3.

1.2. Main applications of optical remote sensing in urban environments

Since their arrival, HR and VHR sensors have been used for a wide range of applications:

- mapping land cover/land use (LCLU), revisiting and updating maps: this is most needed in developing countries, although it is still used elsewhere;
- urban mapping and planning: optical imagery must contribute with additional information that is not provided by databases and must be in accordance, geometrically and semantically with the rules of urban planning;
- land cover (LC) mapping and its evolution dynamic. There has been a significant revival in the use of these applications through modeling and the development of evolution scenarios.

More recently, the study of ecosystems has concerned itself with the challenges posed by sustainable development and biodiversity:

– some of these elements tend to be considered within the framework of the quality of ecosystems, habitats and general resources. This quality is determined by the surfaces and the natural or semi-natural components (vegetation strata, urban waste ground, river banks and waterways, etc.) but also using calculations of biomass [AVI 11, AVI 12, HER 11], storing or capturing carbon, the detection and deterioration of environments or their dispersion [MUR 13], etc. The image is then combined with ancillary data and/or used as an input variable in various models or methods of analysis;

– optical imaging has also recently been used to meet the demands of energy transition such as the thermal evaluation of buildings, identifying rooftops that are optimal for the installation of solar panels or the detection of new construction materials.

The various kinds of available optical technology, such as VHR, hyperspectral or infrared cameras, provide a wide range of possibilities for monitoring the urban socio-ecosystem. Three examples of such applications are outlined in the following sections, with reference to different imaging techniques:

- urban planning by using high spatial resolution imaging devices;
- biodiversity, especially green and blue belts and urban vegetation using spectral imaging devices in the reflective domain;
- monitoring heat islands using thermal infrared imaging.

1.2.1. The use of very high spatial resolution multispectral imaging (VHR) for urban mapping and planning

LC databases have been compiled at different levels (worldwide, European, national, regional and local) in order to meet societal, regulatory and scientific demands. Describing LC makes it possible to produce environmental indicators for the management of ecosystems and territories, especially for urban areas. Thus, an up-to-date LC database makes it possible to study territorial evolutions and to monitor certain natural or anthropic phenomena in order to implement related public policies related. These data are then used to evaluate the impact of these policies. A good example of the way in which this is used relates to territorial urbanization [DUP 12, SU 11,

PHA 11], with the monitoring of artificial sprawl and urban densification. Another example concerns the study of the spread of vegetation and how it has evolved in urban environments [ZHO 08, DEL 08, LAN 09, PHA 12]. Data regarding LC is also used for planning purposes, particularly within the framework of impact studies, where decisions are taken regarding important building sites, for example. Finally, LC data can be used as an input for climatological or hydrological simulations.

1.2.1.1. *Land cover databases*

The specifications of a LC database, especially for an urban environment, will relate to:

- its geometric accuracy, i.e. the minimal size of objects to be represented for each degree of classification legend. The minimal mapping units (MMUs) are defined by class;
- its semantic accuracy, i.e. the level of detail in its classification legend.

The classification legend of LU is most often organized hierarchically, ranging from fairly general classes to finer subclasses (for example, a general class called “artificial territories” might include a subgroup “communication networks”, where third-level subgroups on roads and paths would be found).

In terms of LC, it is possible to distinguish between land cover (the description of elements without predicting their function) and LU (the role played by certain areas in terms of economic or human activity). For example, what would be termed a built-up area in terms of LC could be residential, commercial or industrial in terms of LU.

Data for LC in urban environments have therefore been compiled at different scales in order to meet different needs. The data are produced using photo-interpretation or semi-automatic techniques which require a phase of correction and validation by photo-interpretation. Existing LC databases describing urban environments will be presented in the following section, ranging from the general to the more specific. These databases are different in terms of their classification legend, their scale of use and the extent of the covered areas.

A summary is presented in Table 1.6.

1.2.1.1.1. European scale: Urban Atlas

The Urban Atlas database was created by the EEA as part of the European Copernicus program. It concerns exclusively the largest urban areas in Europe. The aim of Urban Atlas is to develop a shared terminology for every city in Europe in order to be able to easily compare them in a rigorous manner or to calculate relevant indicators (Figure 1.7).

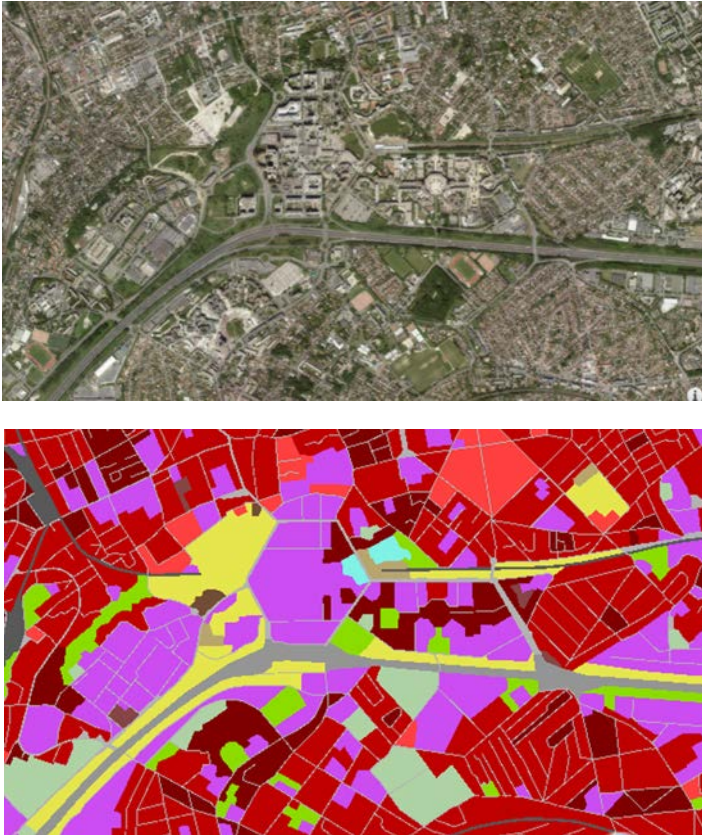


Figure 1.7. Extract from the land cover database Urban Atlas [source: EEA] (above: corresponding orthoimage [source: IGN])

Two versions of the Urban Atlas database exist. The 2006 version dealt only with urban areas with a population greater than 100,000, while the 2012 version was extended to cover urban areas with a population greater than 50,000.

The minimal mapping unit for Urban Atlas was set at 0.25 ha, with a minimal size of 10 m for longer objects. Urban Atlas was produced using satellite images with a resolution of 2.5 m and topographical maps with a scale of 1:50000.

The classification legend of Urban Atlas is hierarchical, featuring three levels and a total of 17 different classes.

1.2.1.1.2. National scale: IGN's large-scale land cover database

In France, IGN¹²'s large-scale LC database (*Base de Données d'Occupation du Sol à Grande Echelle* or BD OCS GE) is still being compiled¹³. With a metric level of accuracy and compatible with the other layers of the national geographic database (*Référentiel à Grande Echelle* – RGE), its purpose is to provide a new component of the large-scale reference geodatabase RGE.

The OCS GE is composed of two levels, one dealing with LC and the other with LU and each has its own hierarchical classification legend. For LC, they include four levels with a total of 14 different classes. The minimal mapping unit varies between 0.5 (particularly for built-up areas) and 2.5 ha.

The BD OCS GE (Figure 1.8) is produced by integrating existing data while also calculating new information from available data, before correcting and completing the process through photo-interpretation.

1.2.1.1.3. Regional scale: land cover in Ile-de-France

LC data Mode d'Occupation des Sols (MOS), provided by the Institute for urban planning and organization (*Institut d'Aménagement et d'Urbanisme* – IAU)¹⁴ in Ile-de-France is one of the oldest databases relating to LC and also one of the most accurate, semantically and geometrically. In use since 1982, it was compiled through the photo-interpretation of aerial images and there have been eight different versions (1982, 1987, 1990, 1994, 1999, 2003, 2008 and 2012).

12 IGN: French National mapping agency.

13 IGN's OCS GE project began in 2012. Compiling the database is carried out in partnership with local organizations.

14 Paris based organization that consults on urban development.

Its legend is hierarchical divided into four levels, with the most detailed level containing 81 different classes. However, this classification legend mostly addresses LU (Figure 1.9).

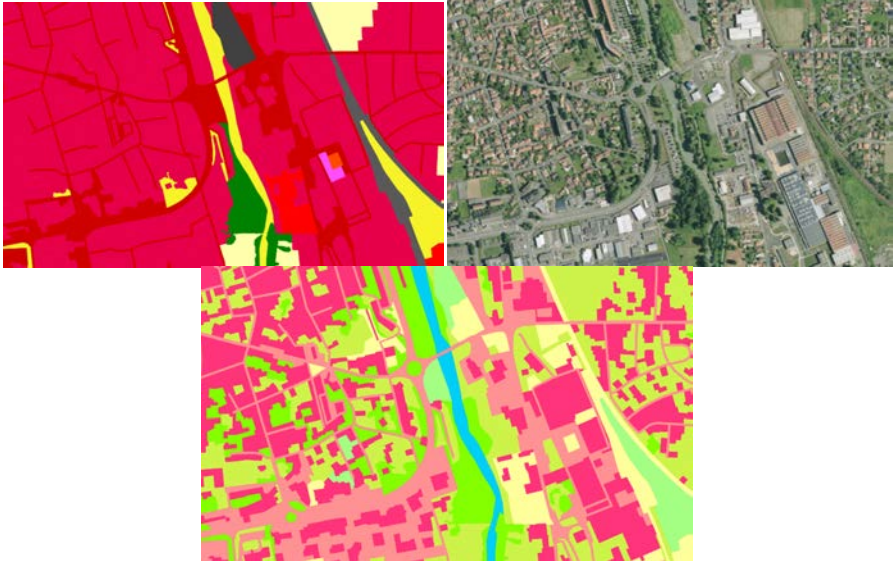


Figure 1.8. Extract from IGN's large-scale land cover database. From top to bottom – land cover, orthoimage of land cover and land use (source: IGN), For a color version of this figure, see www.iste.co.uk/baghdadi/5.zip



Figure 1.9. Land use data for Ile-de-France (for the same area as Figure 1.7) (source: IAU-IDF) For a color version of this figure, see www.iste.co.uk/baghdadi/5.zip

For urban planning purposes, the classification legend of the LC database must be as detailed as possible and includes the different types of urban objects (Table 1.6). These objects are then mapped in order to produce an inventory at a given date, but also to study their evolution. Within this framework, very high spatial resolution multispectral imaging (VHR) is able to produce submetric images, at least in panchromatic mode. At this spatial resolution, it is possible to clearly delineate useful urban objects and to improve how their classification in dense urban areas. It is therefore possible to extract urban objects using VHR multispectral optical data, especially when using supervised methods of classification.

Database	Version	Scale	Minimal mapping unit	Number of levels of classification	Number of classes	Data and production techniques
Urban Atlas	2006, 2012	Europe	0.25 ha	3	17	<ul style="list-style-type: none"> –Photo-interpretation and supervised classification –Satellite image 2.5 m –Topographic map 1:50000
OCS GE (land cover)	Still being compiled, varies depending on the region	France	0.25-2.5 ha	4	14	<ul style="list-style-type: none"> –VHR aerial (or satellite) orthoimages – Integration of existing databases – Photo-interpretation
Land use (MOS)	1982, 1987, 1990, 1994, 1999, 2003, 2008 and 2012	Ile-de-France	Undefined (<500 m ²)	4	81	<ul style="list-style-type: none"> – Aerial orthoimages – Topographic map – Photo-interpretation

Table 1.6. *Main characteristics of different urban land cover databases*

1.2.1.2. Classification techniques using VHR multispectral images

Given a typology of useful urban objects (such as the one in Table 1.1), supervised classification appears to be a technique that is well suited for mapping LC. This consists of training a classifier model using learning data.

These data are collected for each separate class through photo-interpretation, collected *in situ* or taken from existing databases, and it is characterized by spectral, textural or geometric information. A classifier model is calculated from these data and then makes it possible to predict the class of each observation (pixel or region) taken from the image. The model is therefore applied to the whole image in order to produce a LC map. Changes can then be detected by comparing this most recent version to a previous database in order to complete it, update it or to monitor a phenomenon over time.

The operational extraction of LC takes place over several stages described in Figure 1.10:

- calculating the image’s spectral and textural features;
- extracting training areas either manually or using an existing database (especially when used for change detection);
- training: estimating the classifier model using training data and calculated attributes;
- classification: either by pixel or by region;
- detecting changes by making a comparison between the classification and the database requiring an update.

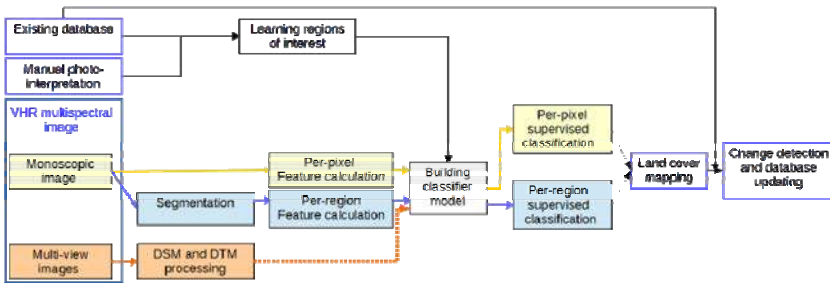


Figure 1.10. Framework for classifying land cover and detecting changes in urban environments. In yellow: the pixel approach; in blue: the object approach; in orange: specific approach for multi-view images (source Bordeaux INP) For a color version of this figure, see www.iste.co.uk/baghdadi/5.zip

Variations to this framework exist depending on whether or not the object concept is taken into account and whether the imagery is monoscopic or multi-view. Indeed for VHR imaging, it can be useful to segment the image in homogeneous regions before moving directly to the classification of these

regions, which are also called superpixels: this is referred to as Object Based Image Analysis (OBIA) [BLA 10]. Where multi-view data is available, a DSM (i.e. an image which connects each pixel to its altitude) can be calculated and used as an input for classification, greatly improving the accuracy classification especially for the discrimination of ground and above-ground objects.

The most widely used classifiers in remote sensing are neural networks [PAI 15], the maximum likelihood, support vector machines (SVMs) [PAL 05] or random forests [BRE 01].

For large-scale processing, the process can be applied by tiles.

Figure 1.11 shows examples of data produced from Pléiades VHR images.

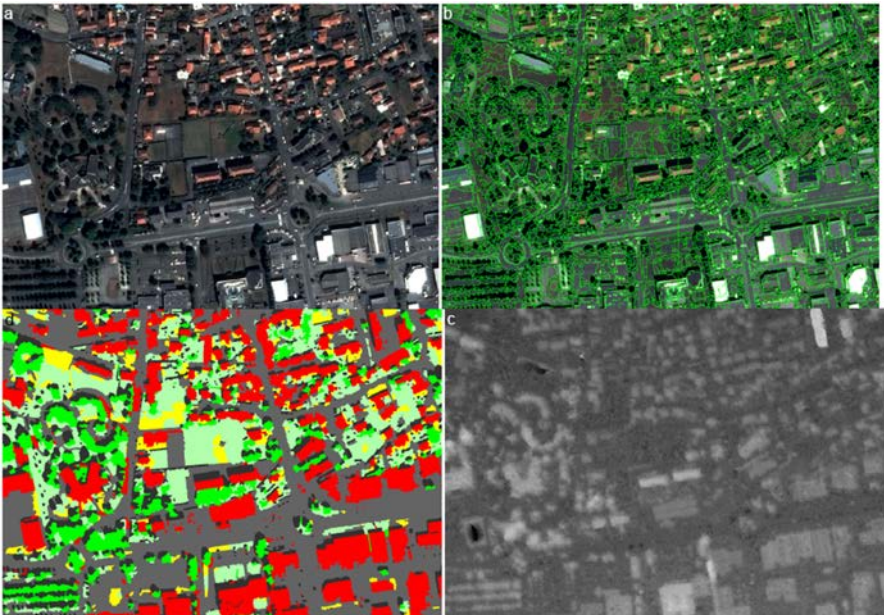


Figure 1.11. Examples of data produced from two Pléiades images (in Tarbes, France): a) resampled and pansharpened orthoimage at 50 cm, b) an example of segmentation, c) Digital Surface Model (increasing altitudes from black to white) and d) an example of classification (shadows in black, buildings in red, road networks in gray, bare earth in yellow, high vegetation in bright green and low vegetation in pale green) (source: IGN). For a color version of this figure, see www.iste.co.uk/baghdadi/5.zip

1.2.1.3. Feature calculation and selection

Whether an object-based or pixel-based approach is adopted, the classifier does not necessarily use the initial bands of the multispectral image, but transformed channels calculated from the initial bands (most of the time red – green – blue – near-infrared) of the image. These derived channels make it easier to distinguish certain classes, as is the case with the spectral index NDVI (Normalized Difference Vegetation Index) which is used to detect vegetation. There are several different kinds of these derived channels, or neo-channels, also known as features in case of classification:

- spectral features: these are the spectral indices such as the vegetation indices [HEN 12], brightness indices, water indices or bands transformed in another colorimetric space (Intensity/Hue/Saturation or $L^*a^*b^{15}$ spaces, for example) or all other indices obtained by a simple combination of initial bands;

- textural features: these are calculated at the pixel level (by integrating the information within a given neighborhood) or at the regional level (if we have access to a segmentation) and characterize the image's textural information (structure, roughness, contrast, etc.). We can cite, for example, the textural indices of Haralick [HAR 73] or Gabor [GRI 02], the morphological attribute profiles [DAL 10] or approaches based on descriptors such as the Histogram of Oriented Gradient or HoG [DAL 05];

- geometric features: features which are specific to the object-based approaches, outlined in section 1.2.1.4.

The use of well-suited derived channels often makes it possible to improve classification and to better distinguish between different classes. Selecting these features is highly important and will affect the accuracy of LC classification.

With this in mind, automatic feature selection methods can be used in order to identify optimal sets of features. Sometimes, these will be dependent on the classifier [GUY 02, BRE 01].

¹⁵ The $L^*a^*b^*$ color space includes all perceivable colors. Three figures characterize the colors: *lightness* L which is derived from the radiance and two parameters a and b which express the difference between the color and a gray surface of the same brightness.

1.2.1.4. *The contribution of object-based classification*

The pixel-based approach is easy to implement but has a tendency to lead to noisy classification. This then requires postprocessing in order to regularize the result in a given neighborhood to obtain a LC map. In order to solve this problem, different regularization techniques have been proposed. They include local, filter-type approaches such as majority vote or bilateral filtering [TOM 98], or more general methods based on probabilistic graphic models solved owing to optimization methods such as graph cuts [SCH 12].

This phenomenon is much more sensitive in the case of VHR imagery, to the extent that the same object will be represented on the image by several pixels. It is therefore worthwhile carrying out joint processing on different pixels which correspond to the same object. This kind of processing requires an image segmentation.

Image segmentation divides an image into a group of homogeneous regions, which are disjoint from each other and their union forms the whole image. For segmentation, the parametrization choice can be critical, given that the aim is to have regions which are of a significant size and where the LC is consistent. Fine- or oversegmentation will contribute little in relation to classification carried out per pixel and will run the risk of leading to noisy classification, while undersegmentation, that is to say a segmentation that is too coarse, containing regions of different classes, will also lead to misclassification.

Various segmentation algorithms have been put forward, for example, [BAA 00, BEN 04, COM 02, GUI 06] and [ARB 11].

Regions created by segmentation can be used within the framework of a regularization process as for pixel-based classification. However, an object-based classification approach will use the segmented regions as input and derive specific object features [MAT 07, ZHA 10, MYI 11] and will immediately provide a less noisy classification. Examples of these objects features include:

- statistical features within the region (calculated from pixel-based features);
- geometric features describing the regions' shape;

– contextual features: these features take the local context into account. For example, the neighboring region of a shadowed area in the direction of the sunlight will most likely be above ground.

The use of segmentation therefore makes it possible to obtain a more smooth classification, but we have to keep in mind that there is a risk of error spreading from segmentation to classification.

Figures 1.12 and 1.13 show the regularization and improvement in classification through the object-based approach, especially for roads which are often confused with buildings. Object classification is more even but still leads to significant confusion when trying to distinguish between asphalt roads and asphalt roofs.

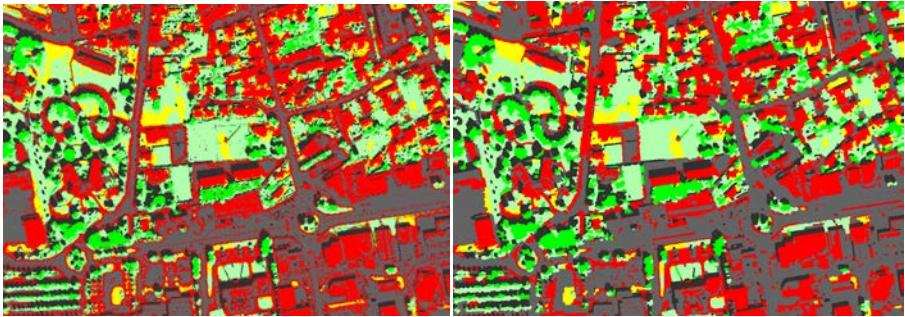


Figure 1.12. Classification by maximum likelihood classifier by pixel a) and by region without using a Digital Surface Model b) (source: IGN). For a color version of this figure, see www.iste.co.uk/baghdadi/5.zip

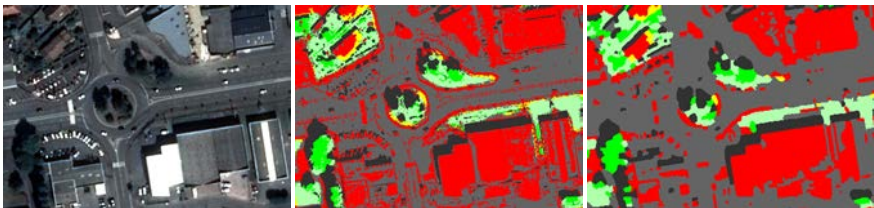


Figure 1.13. Examples of classification by maximum likelihood classifier by pixel (center) and by region (right) taken from a Pléiades ortho-image (left) (source: IGN). For a color version of this figure, see www.iste.co.uk/baghdadi/5.zip

1.2.1.5. Contribution of digital surface models in urban classification

The development of VHR satellite imaging in tandem with increased satellite agility (as is the case with the Pléiades sensor) has made it possible to acquire images in stereoscopy and even tri-stereoscopy without diachronism while. Aerial VHR acquisitions are almost always multi-view (more than three images). One of the advantages of multi-view VHR imaging is that it enables the calculation of DSMs with submetric resolution, i.e. a 2.5 D representation of the image, where the value of each pixel reflects its altitude on the terrain while taking into account objects above the ground (buildings, vegetation, etc.).

Such DSM are calculated using dense automatic correlation image matching techniques [PIE 06, GRA 11]. In urban environments, filtering techniques, for instance using an elastic grid algorithm [CHA 06], can then be used to delete above-ground objects making it possible to produce a digital terrain model (DTM), that is to say a grid of altitudes at ground level. It then enables us to derive from such data whether an object is at ground level or above for each pixel as a function of the difference between the DSM and the DTM. This difference is called normalized DSM (nDSM) and makes it easier to distinguish between classes which are spectrally similar such as roads and buildings with gray roofs on one hand and areas of bare ground areas and some red-tiled buildings on the other hand.

Depending on the type of classifier used, these data are either taken into account directly as new features based on the difference between the DSM and the DTM and provided as an input to the classifier or as *a priori* probabilities of classification given the difference between the DSM and the DTM. These probabilities are then merged retrospectively with posterior classification probabilities produced by the classifier through Bayesian [LEB 11] or fuzzy [ROT 07, POU 09] data fusion approaches. An example of ground versus above-ground probability classification described using a piecewise linear function is shown in Figure 1.14.

Figures 1.15 and 1.16 illustrate the benefit of using DSMs when classifying by pixel or by region. Ambiguities which were presented in Figure 1.12 have been removed by distinguishing between ground and above-ground objects.

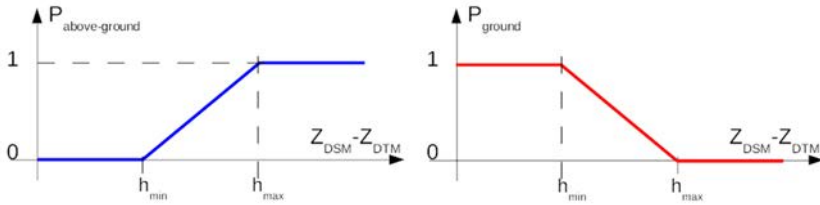


Figure 1.14. Probability of being classified as ground level or above-ground level as a function of the difference in altitude between the DSM and the DTM (source: IGN).

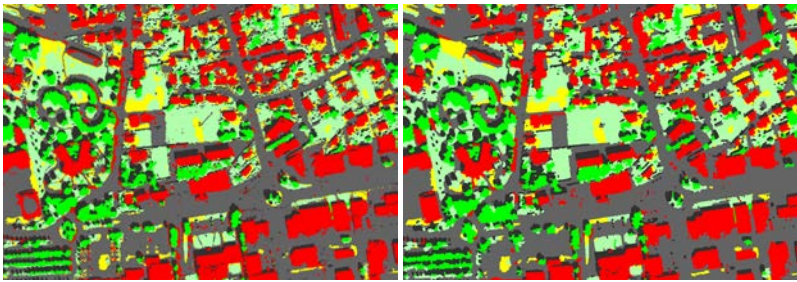


Figure 1.15. Classification by maximum likelihood classifier using DSM, by pixel a) and by region b) (source: IGN). For a color version of this figure, see www.iste.co.uk/baghdadi/5.zip

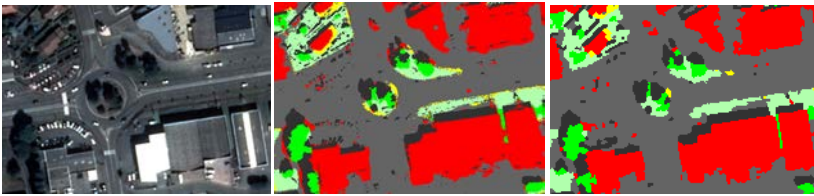


Figure 1.16. Examples of classification by maximum likelihood classifier using DSM by pixel (center) and by region (right) on an extract from a Pléiades orthoimage (left) (source: IGN). For a color version of this figure, see www.iste.co.uk/baghdadi/5.zip

1.2.2. Biodiversity (blue belt and green belt) and vegetation detection in cities

Despite a blurring of the concept [GUY 08], biodiversity, or at least the biological diversity of species found in cities [PRE 08], has taken on

significant social, economic [MAR 06] and legal dimensions. The delicate balance between cities and the natural world is constantly changing, in part due to work carried out as part of the Millennium Ecological Assessment [MEA 05] which highlighted the challenges facing biological diversity and especially the strong ties between urban development and the health of ecosystems. In reality, “changes caused by anthropic activity have happened more quickly over the course of the last fifty years than during any other period of human history” [MEA 05]. Those transformations that have been observed are linked to the conversion of natural ecosystems into socio-ecosystems dominated by humans. Urbanization has had a negative effect on biological diversity and has caused the destruction of habitats by using these natural environments for various projects (construction, extraction, fragmentation and expansion), but it has also helped its development by creating specific zones – wildlife corridors, green belts, plants on roofs and walls, protected zones, etc. Green and blue belts can therefore be thought of as sites of both biodiversity and construction which spread across cities; they play an important role in the ecological functioning of species in this mostly mineral environment alongside existing vegetation (parks, gardens, rows of trees, etc.). In urban environments, biodiversity is localized depending on the different types of habitat (ground surfaces, vegetation, water and increasingly roofs and walls, trees or building), following the permeability gradient of the matrix and urban density. Vital for one or several species, these habitats are very diverse and are constrained by the urban matrix. They correspond to natural infrastructure that is necessary for the displacement of fauna and the dispersion of flora, but also for their reproduction, protection, feeding and rest.

Among this diverse range of infrastructures is where wildlife corridors are to be found. These natural or protected areas were set up following the application of the Habitats Framework Directive¹⁶ and were extended in urban environments by clearly defining green and blue belts. In France, the implementation of green and blue belts since 2007 has been one of the major national projects to come from the Grenelle Environment Forum. This belt is made up of a network of biological corridors (or ecological corridors, existing or to be restored), “biodiversity reservoirs” and buffer zones or annexes (“natural relay spaces”). Documents provided by state services make it possible to identify these structures and to map them for town

16 Directive 92/43/CEE of the Committee on 21st May 1992 regarding the conservation of natural habitats as well as wild flora and fauna.

planning purposes using satellite data¹⁷. At the European level, protocols for evaluating and mapping ecosystem services have been studied and put forward by the European Commission, drawing on a range of data sources (Figure 1.17).

<i>Mapping ecosystems</i>	
<i>Urban</i>	Land use land cover data, e.g.
<i>Cropland</i>	Corine Land Cover
<i>Grassland</i>	Copernicus high resolution data
<i>Woodland and forest</i>	Elevation data
<i>Heathland and shrub</i>	Seabed maps
<i>Sparsely vegetated land</i>	National datasets
<i>Wetlands</i>	
<i>Rivers and lakes</i>	Models for spatially delineating wetlands or
<i>Marine inlets and transitional waters</i>	natural, unmanaged ecosystems
<i>Coastal</i>	
<i>Shelf</i>	
<i>Open ocean</i>	

Figure 1.17. *Mapping ecosystems* (<http://biodiversity.europa.eu/>)

Within the context of mapping habitats or the conservation of natural spaces, remote sensing makes it possible to identify, quantify and even model them. The data can also provide information on stress (in particular hydric stress, but also irradiance, constraints on the tree crown, etc.) and on the health and well-being of species. Spatial and spectral resolutions are key elements in these observations. Thus, satellite imaging has been used in order to establish continuity at a regional level (Regional schematic of ecological coherence (*schéma régional de cohérence écologique* – SRCE)): ecological continuity [HUB 12], wooded [VAN 11] or semi-natural environments [FAU 14].

In a similar manner, preserving ecological continuities and ensuring their quality incorporates a range of different activities in the sphere of environmental preservation, such as classified or unclassified wooded areas or even the development of waterproof surfaces or wetlands [RAP 12]. Such

17 Directed by the French Ministry for ecology, sustainable development and energy (MEDDE), the TVB Resource center is based on an umbrella organization which brings together Aten, the French federation of regional natural parks, the national institute for studies in science and technology for environment and agriculture (Irstea), the Museum of Natural History (MNHN) and the national office for water and aquatic environments (Onema).

environments facilitate hydric transfer and act as buffer zones against the risk of flooding [WEN 12, KAS 15].

In studies focused on urban biodiversity, particular attention has been paid to vegetation. It has been identified as a key element for quality of life in cities and reinforces the benefits of urban living [BON 06, VAN 03]. Urban vegetation is currently a key aspect of political agendas. Aside from monitoring ecological continuities or forests and parks, the aim is to be able to isolate and identify the relevant areas in order to characterize the evolution of these habitats within the urban belt [PUI 14, ROU 14, BOU 10, MAI 12] (Figure 1.18).

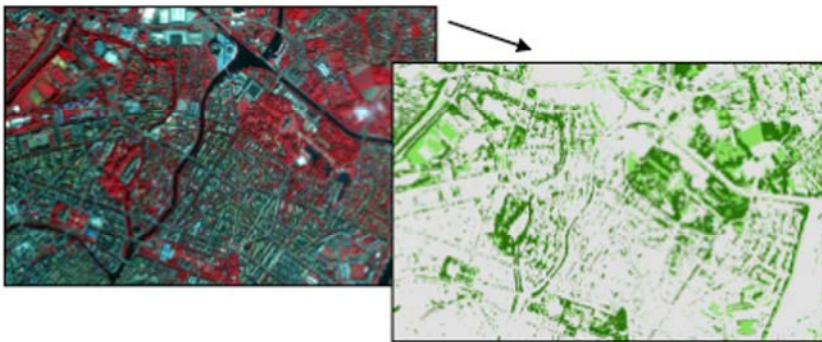


Figure 1.18. Extraction of trees and shrubs using VHR images (Pléiades) [ROU 14]. For a color version of this figure, see www.iste.co.uk/baghdadi/5.zip

Repeatable, generic methodological propositions for analysis using multi-source data are currently being developed in order to characterize urban spaces. Iovan *et al.* [IOV 08] and Ardila *et al.* [ARD 11, ARD 12] focused on the detection of tree crowns by using an object-oriented approach. Other developments based on training algorithms (Random Forest) currently make it possible to improve the detection and identification of trees in urban environments [PUI 14].

Over the course of the last decade, various initiatives have been introduced in order to promote green or open spaces [JOH 04]. Urban vegetation plays an essential role in the management of environmental characteristics such as wind, humidity and solar irradiance [GIV 98]. Thermal comfort is in correlation with the presence of vegetation [GOM 04, GUL 05] namely due to

its capacity to reduce temperature through shadow (direct effect), heat islands and evapotranspiration (indirect effect). Large or dense areas are more effective than a few narrow or less dense areas [STU 90, DIM 03]. As a result, vast areas can be used in order to help cool down the air in the city, which can be felt far from the direct localizations of vegetation, namely, through cooling islands [SHA 00]. Through the quality of the information provided, hyperspectral imaging is an asset for analyzing the ecological diversity of vegetation [WAN 07b, GAN 08, BLA 06a, BLA 06b].

1.2.3. Urban heat islands

1.2.3.1. Introduction to the concept of heat islands

Studying urban areas through thermal infrared remote sensing (LWIR, long-wavelength infrared: 8–14 μm) dates back to the 1970s and studies carried out by Rao [RAO 72] and Carlson *et al.* [CAR 77]. There are currently three problems being studied using this technology [VOO 03]:

- the link between the spatial structure of urban thermal patterns and the characteristics of the urban surface;
- the energy balance of urban areas;
- urban heat islands (UHIs), a concept that will be explained here.

The following section will focus on this last point. Urbanization implies the replacement of natural surfaces by artificial materials, which possess different physical properties. This transformation causes changes in the area's climate characteristics and one of these is the UHI effect [OKE 81]. This phenomenon can be characterized as the warming of built-up zones in relation to surrounding, undeveloped areas. Oke [OKE 81, OKE 82] lists the main causes of UHI, which were then dealt with by Voogt [VOO 02]:

- geometry: solar irradiance is trapped in urban canyons which causes multiple reflections;
- the characteristics of urban materials: these materials have an increased thermal capacity and therefore store more heat than natural materials. Furthermore, these materials are insulating as well as being waterproof which reduces evaporation and thus warms the surrounding air;
- anthropogenic heat: human activity, particularly the energy output of buildings and vehicles, produces heat.

– contamination: urban areas are the main sources of greenhouse gas emissions.

The UHI effect can have negative as well as positive effects. In the first instance, one example is the direct influence it has on health and well-being. The effects of rising temperatures range from causing sleep problems to an increased mortality rate [BRU 05]. In the second instance, one example of the positive impact is with cold cities where rising air temperatures decreases the need to heat homes and, as a result, reduces energy consumption.

Characterizing UHI using weather stations is insufficient because they are not able to cover the entire urban area in a consistent manner. In contrast, remote sensing provides us with an instantaneous image of the entire city. Thus, UHI can either be defined at the atmospheric level or at the surface level. Atmospheric UHI depends on the position of the air temperature sensors: either in the urban canopy, i.e. using the air temperature measured between the road and the roofs, or in a boundary layer, situated above the preceding layer. Surface UHI on the other hand (referred to from now on as SUHI) is studied using remote sensing data and the parameter to be estimated is not the air temperature but the land surface temperature (LST):

$$SUHI = LST_{urban} - LST_{rural} \quad [1.3]$$

where LST_{urban} refers to the surface temperature of the urban area and LST_{rural} refers to the surface temperature of the rural area. In order to estimate the SUHI, several stages of processing are necessary. The aim of the first stage is to estimate the materials' emissivity (section 1.2.3.2), followed by a second phase where the surface temperature is estimated (section 1.2.3.3). Finally, examples of SUHI studies are provided (section 1.2.3.4).

1.2.3.2. *The surface emissivity of urban areas*

In urban environments, an accurate estimation of the surface temperature¹⁸ depends on surface characteristics and in particular its emissivity and geometry [VOO 03]. Thus, an uncertainty of 1% for the emissivity leads to an error of 0.78 K for temperature estimating [VAN 93]. In addition, due to its heterogeneity, an accurate estimation of emissivity is

18 The problem of estimating the surface temperature and emissivity is outlined in [BRI 16].

essential in order to deduce a temperature map in urban environments, which will be used in order to quantify the city's SUHI.

In [OLT 12], three methods for estimating emissivity are compared in order to create a map of surface temperature using data acquired by the hyperspectral scanner AHS (Airborne Hyperspectral Scanner) during the European Space Agency (ESA) mission DESIREX 2008 over the city of Madrid [SOB 13]. The results show that with these three methods, emissivity is estimated with a precision of 5.6% for the Normalized Difference Vegetation Index Threshold Method (NDVI_{TM}) [SOB 08], 3.0% for the TISI (Temperature Independent Spectral Indices [BRI 16, BEC 90] and 3.9% for TES (Temperature-Emissivity Separation [BRI 16, GIL 98]. However, there are operational disadvantages to all three methods. Even if the NDVI_{TM} method is used in urban environments [RIG 06, STA 07], it is limited by the reduced number of classes of material that it takes into account (three classes: vegetation, bare ground and mixed pixels). The TISI method requires a channel in the mid-wavelength infrared (MWIR: 3–5 μm) as well as multitemporal acquisitions. Finally, the TES method developed for ASTER requires at least five bands in the low-wavelength infrared region (LWIR). Furthermore, the TES method is an empirical method and can lead to an error of 1.7% for emissivity [OLT 14] if urban materials are not taken into account during calibration.

A fourth method for mapping emissivity in urban areas is put forward by Sobrino *et al.* [SOB 12a]. A ground classification map (12 classes) is compiled using 80 AHS bands which cover the entire spectrum, from 0.4 to 13 μm . In order to associate with each class an emissivity spectrum, the ASTER database is used combined with field measurements. For devices with weak spectral resolution in the LWIR, this would appear to be the most promising method. The urban environments have slow temporal evolutions (apart from vegetation) and a map of materials (buildings, infrastructures, etc.) can be obtained from external high spatial resolution images in the reflective range. Then, the corresponding emissivity for each class will be chosen from a spectral library.

1.2.3.3. *Land surface temperature in urban areas*

Obtaining the land surface temperature, LST in urban environments is linked to the acquisition geometry of the 3D structure of the scene.

Furthermore, the temperature measured for an urban area shows significant daily directional effects, due to a city's high thermal heterogeneity (surfaces in shadow or in sunlight) and the directional properties of urban materials [LAG 04]. These phenomena are illustrated in Figure 1.19 which shows two temperature maps obtained using the TES algorithm [GIL 98] for two acquisitions of the AHS sensor during the ESA mission DESIREX 2008 [SOB 13], over the city of Madrid. The spatial resolution of the maps is 4 m and the AHS device has a field of view of 90°. Figure 1.19 corresponds to an acquisition carried out from the North West (NW) to the South East (SE) and Figure 1.19(b) corresponds to an acquisition across the same region but along the South (S) – North (N) axis. Both were acquired around midday local time with the second carried out at an interval of 20 min in relation to the first. There is a difference in temperature between the two maps, caused by the different surfaces viewed by the sensor depending on their position in relation to the sun. More shadows are observed when the city is covered in a NW to SE direction than when it is covered in an S to N direction. However, toward midnight, with the same acquisition configurations, any difference between the two flight lines disappears (Figure 1.20). This shows that it is easier to analyze urban environments at night in order to study urban heat islands [SOB 12b].

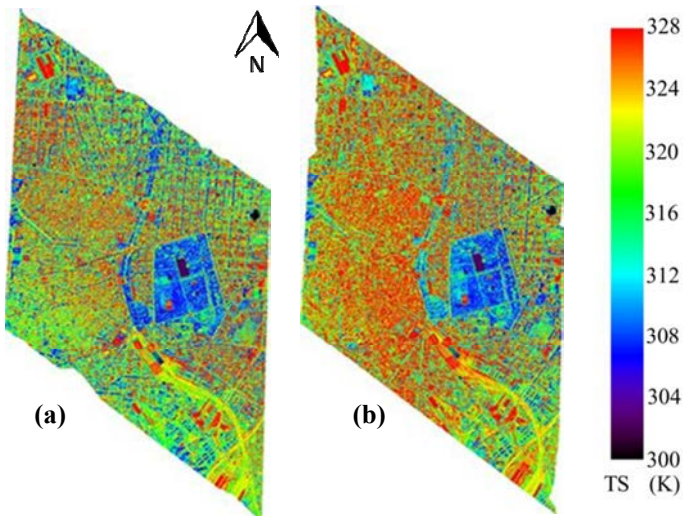


Figure 1.19. Land surface temperature maps for the same area of Madrid at midday: a) transect from NW to SE; b) transect from S to N [OLT 13]. For a color version of this figure, see www.iste.co.uk/baghdadi/5.zip

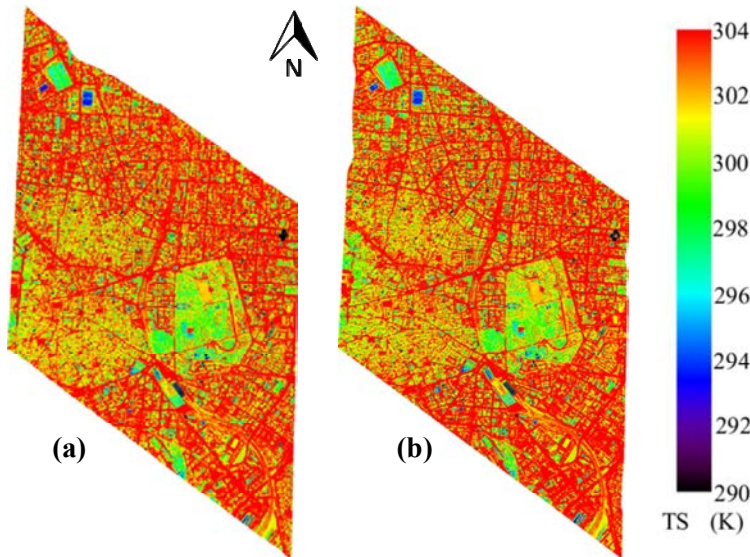


Figure 1.20. Land surface temperature maps for the same area of Madrid at midnight: a) transect from NW to SE; b) transect from N to S [OLT 13]. For a color version of this figure, see www.iste.co.uk/baghdadi/5.zip

The SUHI effect is studied in the bibliography using satellite and airborne sensors. One example of an airborne mission is the DESIREX mission, where the SUHI for Madrid is characterized during the summer with a maximum of 5 K [SOB 13].

The satellite devices currently in use do not possess a spectral or spatial resolution adapted to studying urban environments. However, they do offer a more cost-effective alternative to airborne acquisitions and are capable of providing temporal monitoring of the SUHI. Thus, the device MODIS, with a spatial resolution in the LWIR frequency of 1 km, was used by Bonafoni *et al.* [BON 15] in order to monitor the evolution of SUHI for the city of Milan (Italy) over the course of a day, using four MODIS acquisitions per day. A difference of more than 4 K can be observed between the diurnal and nocturnal SUHI. Various studies using ASTER images (a spatial resolution of 90 m and five spectral bands in the LWIR frequency) have also been carried out in order to characterize the SUHI, an example of which is shown in Figure 1.21. This image shows a temperature map for Madrid at night, where the city can be identified by its high temperatures (in red) compared to the surrounding area. In [TIA 08], LST maps obtained with

ASTER at night are compared to air temperature measurements for Grand Manilla (Philippines). The maximum SUHI registered there is 3 K and there is a linear correlation between LST and air temperature, with a correlation coefficient of 0.55.

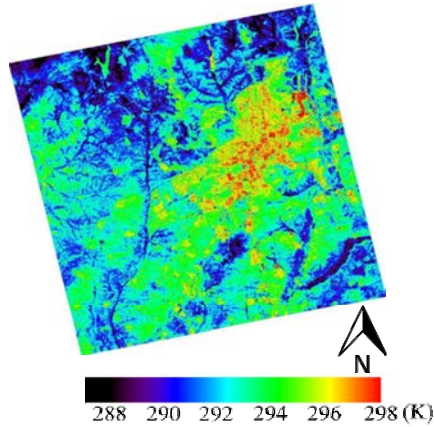


Figure 1.21. Land surface temperature map for the night of 4 July 2008 obtained using the TES algorithm [GIL 98] using an ASTER image of the city of Madrid and its surrounding area. The SUHI effect can be observed [OLT 13]. For a color version of this figure, see www.iste.co.uk/baghdadi/5.zip

Atmospheric UHI is characterized by higher levels at night and very weak, sometimes negative, levels (urban cooling islands) during the day, due to the shadows caused by buildings and urban vegetation. In the case of SUHI, we are able to note the same results for other cities such as Athens [STA 09] or Madrid [SOB 13]. However, SUHI does not always show this dynamic and it is possible to find examples where SUHI is more intense during the day than at night [BON 15]. Furthermore, this dynamic can change during the year, because the effect is linked to land cover. Even if there is no remarkable change to urban surfaces over a year, this is not the case for the surrounding areas of cities where agricultural activity, for example, can bring about seasonal changes in the surface cover. Figure 1.22 gives an example of this dynamic for the city of San Miguel de Tucuman (Northwestern Argentina), with the SUHI calculated using Landsat TM images at 2pm UTC [OLT 10]. We were able to observe a positive SUHI during the summer and a negative SUHI during winter and spring, with these results caused by crop conditions around the city, particularly sugar cane.

During September, October and November, when the SUHI is negative, the proportion of bare ground in the pixels which cover sugar cane crops is higher than during January, February and March, when sugar cane leaves are greener and more developed. As a result, for the first case, the rural surface at 2pm is warmer than the urban surface, while for the second case the inverse is true.

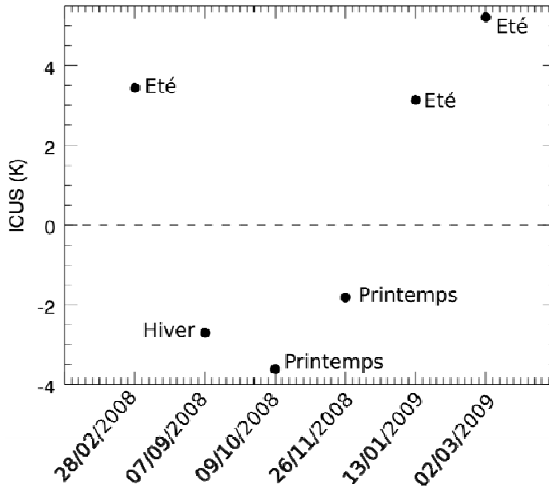


Figure 1.22. SUHI measured using Landsat TM images (2pm UTC) for the city of San Miguel de Tucuman (Argentina) [OLT 10]

1.3. Conclusions and prospects

Urban environments are characterized by a very high spatial heterogeneity in terms of materials, which requires remote sensing methods with high spatial resolution (lower than 5 m) and high spectral range in the optical domain.

From a methodological point of view, there will be need for research developments on the data processing level and the use of the available big data.

At the level of data preprocessing, studies which aim to improve atmospheric correction in the optical domain will need to be pursued. Developments based on the simultaneous use of data acquired in the reflective domain and the thermal infrared domain should be aided by the

availability of new airborne devices covering the entire optical domain. Furthermore, linear and/or nonlinear separation techniques will need to be developed in order to identify materials at a subpixel level and to thus improve the quality of classification, in the reflective domain as well as the emissive domain.

For the production of LC maps in urban environments through classification, VHR imaging enables access to more detailed geometric data and thus improves the classification of homogeneous regions of LC taken from a segmentation by reducing the noise. Nevertheless, in urban environments, using the image alone leads to limited results caused by the confusion between similar classes. In the case of multi-view acquisitions, it is possible to improve these results by introducing 3D information regarding the height of objects (DSM and DTM).

However, the implementation of such approaches remains limited in the case of satellite imaging given the costly and difficult (in terms of programming) nature of acquiring multi-view scenes. In addition, approaches which combine pattern recognition and classification could make it possible to make better use of the geometric data accessible via VHR imaging in the case of monoscopic scenes [KAR 09, SID 14]. Another possible improvement could come through the use of deep learning methods which are starting to be introduced for geospatial images [MAR 15, MNI 12, PAI 15] after recent successes, particularly for image indexation. Such approaches have become possible due to the availability of significant volumes of learning data, in the case of existing database updates.

The next methodological developments will be based on the following two important points:

- the fusion of multi-source data (optic, radar, LiDAR and hyperspectral) [GUO 11] and multi-sensors (multiple spatial and temporal resolutions) in order to improve the classification of different usable urban objects;
- the use of temporal data for change detection and updating urban databases.

For studying biodiversity, hyperspectral imaging with high spatial resolution is necessary in order to be able to identify a vegetation species. Combining it with 3D data is necessary in order to be able to distinguish high vegetation from low vegetation.

Regarding the study of urban heat islands, there are a number of airborne methods which make it possible to study them at a local level. However, there is no satellite sensor with a sufficient spatial resolution for carrying out such a study. Merging spectral LWIR images with HR or VHR images in the reflective domain is one alternative for separating thermal infrared pixels and to gain a higher spatial resolution. These studies must be pursued with a view toward establishing a connection between the surface temperature estimated through remote sensing and the air temperature in order gain a better understanding of the temperature's directional activity and to establish a connection between remote sensing methods at different levels.

Sensors are constantly evolving. In the domain of satellite imaging, improvements in geometric resolution and the agility of satellites are in progress. At the same time, there has been an improvement in terms of spectral quality, with superspectral sensors such as Landsat-8 or Worldview-3, as well as in terms of the repetitivity of acquisitions over time using microsatellite constellations such as SkyBox. Greater spectral quality allows for a better quality of classification, as well as for a more detailed legend, including studying the state of vegetation or mapping materials, which are useful to model the urban system. High repetitivity of acquisitions over time also makes it possible to study phenomena more accurately, including the state of vegetation again, but also to meet urgent requirements in up-to-date data, in crisis situations or following a natural disaster, for example. In the aerial domain, Unmanned Aerial Vehicle (UAVs) acquisitions continue to be developed, and these have the advantage of a greater level of reactivity and agility, a higher spatial resolution (Ultra-High Resolution (UHR)) and lower costs (over small areas) compared to traditional airborne acquisitions. Their applications will be the same as for airborne acquisitions, but will feature higher resolution, increased accessibility and a wider viewing range. An example of this can be seen in the case of more detailed and more complete 3D architectural modeling which integrates building facades, in the monitoring of the condition of materials and measuring thermal flows. However, the use of UAVs in urban environments remains limited due to flight restrictions in populated areas as well as the significant weight of some of the imaging equipments.

While improvements in equipment and methods can be considered evidence of genuine progress, other barriers continue to stand in the way, including how best to use the wealth of data that are currently available. This

massive amount of data leads us to consider current methods for using data and information. Within this context, there are possible avenues of research which should take into account the representation needs of data for several subjects or users. Metadata will be indispensable for describing selected data in order to meet the various challenges posed by urban ecosystems. Contextual, cognitive and expert information must be taken into account in order to strengthen the link between the image and reality. Finally, the uncertainty and the quality of available data will require to be specification and representation. In order to deal with applications linked to the use of satellite imaging, it will doubtless be necessary to develop a greater degree of harmony among producers, data processors and users while continuing to shape the process in order to satisfy the needs of final users within an intercognitive framework (elected officials, technicians, state representatives, NGO members or ordinary citizens). Formats adapted to users as well as to the different kinds of media used (digital or otherwise) will need to be developed and improved.

In a digital environment that is accessible to the majority of people living in urban environments, representations of urban space are an essential source of reference. Cartographic systems for identification, evaluation and planning are becoming increasingly diverse. Improvements in spatial resolution have made it possible to get closer to the geometric accuracy of equipment used to carry out measurements on the ground. As for needs, they are varied and often unspecified. It is clear that satellite imaging has a role to play, but often it must be accompanied by other sources of information (maps, on-ground data, historical records, etc.) These combinations can follow one of two paths: the relationship between the user and the product (the connection between the image and reality, the connection between the different classification used by users and providers of data) and the relationship between various sources produced using different intrinsic and extrinsic characteristics (between a cartographic element, information found online and the image itself, for example).

With the vast amount of information available on the Internet and in digital form, especially since data started to be considered “common property”, that is shareable, modifiable and able to be used for various purposes and by a number of users, access to the different kinds of geographical data has widened, joining the flow of “open data” available since 2005 and especially since 2008 [PS1 05]. However, despite the

increasing availability of information, questions regarding how accessible it is actually for urban populations continue to be asked.

The future is digital and the heterogeneous dataset available for characterizing urban systems is vast and will only continue to grow. Nevertheless, this does not guarantee the quality of information provided. The speed at which results are transmitted does not guarantee their quality nor does it mean that they will be evaluated in an equivalent manner. Masses of numerical, geographical and environmental data are already available and this will increasingly be the case taking into account current sociotechnical advances and those to come in the future. This will lead to new directions of research in more intelligent data models which will draw together the quality of the original information and the emergence of new knowledge while trying to objectify the relevant uncertainty.

1.4. Key points

In order to gain a proper understanding of the way in which the urban ecosystem functions at a local level, high spatial and spectral resolution optical remote sensing is relevant and necessary. It is relevant because it provides largely stable quality data for large areas with a level of repetitivity that is only going to increase. Furthermore, satellite imaging increasingly provides spatial resolution that is adapted for planning and organization carried out by local authorities.

Finally, the spectral resolution of satellites makes it possible to provide data on chemical compositions, changes and modifications in materials and urban shapes. As such, satellite imaging has become necessary in order to comprehensively cover the required areas, to monitor urban spaces and the effect of urbanization on the environment.

Methodological equipment exists for measuring surface properties: reflectance, emissivity and temperature. Urban remote sensing provides responses for a wide range of applications such as planning, detecting changes, heat islands, material dynamics and biodiversity. LC classification can be adapted to the needs of end users for representing, monitoring or prospective actions. Other products including maps of materials are also possible.

3D information continues to be necessary in order to be able to properly detect different above-ground classes.

1.5. Bibliography

- [ADE 13] ADELIN K.R.M., CHEN M., BRIOTTET X. *et al.*, “Shadow detection in very high spatial resolution aerial images: a comparative study”, *ISPRS Journal of Photogrammetry and Remote Sensing*, vol. 80, pp. 21–38, 2013.
- [ARB 11] ARBALAEZ P., MAIRE M., FOWLKES C. *et al.*, “Contour detection and hierarchical image segmentation”, *IEEE Transactions on Pattern Analysis and Machine Intelligence*, vol. 33, no. 5, pp. 898–916, 2011.
- [ARD 11] ARDILA J.P., TOLPEKIN V.A., BIJKER W. *et al.*, “Markov-random-field-based super-resolution mapping for identification of urban trees in VHR images”, *ISPRS Journal of Photogrammetry and Remote Sensing*, vol. 66, pp. 762–775, 2011.
- [ARD 12] ARDILA J.P., BIJKER W., TOLPEKIN V.A. *et al.*, “Context-sensitive extraction of tree crown objects in urban areas using VHR satellite images”, *International Journal of Applied Earth Observation and Geoinformation*, vol. 15, pp. 57–69, 2012.
- [AVI 11] AVITABILE V., HEROLD M., HENRY M. *et al.*, “Mapping biomass with remote sensing: a comparison of methods for the case study of Uganda”, *Carbon Balance and Management*, vol. 6, no. 7, 2011.
- [AVI 12] AVITABILE V., BACCINI A., FRIEDL M.A. *et al.*, “Capabilities and limitations of Landsat and land cover data for aboveground woody biomass estimation of Uganda”, *Remote Sensing of Environment*, vol. 117, pp. 366–380, 2012.
- [BAA 00] BAATZ M., SCHÄPE A., “Multiresolution segmentation – an optimization approach for high quality multi-scale image segmentation”, in STROBL J., BLASCHKE T., GRIESEBNER G. (eds), *Angewandte Geographische Informationsverarbeitung XII*, Wichmann, Heidelberg, pp. 12–23, 2000.
- [BEC 90] BECKER F., LI Z.L., “Temperature-independent spectral indices in thermal infrared bands”, *Remote Sensing of Environment*, vol. 32, pp. 17–33, 1990.
- [BEN 01] BEN-DOR E., LEVIN N., SAARONI H., “A spectral based recognition of the urban environment using the visible and near-infrared spectral region (0.4–1.1 μm): a case study over Tel-Aviv”, *International Journal of Remote Sensing*, vol. 22, no. 11, pp. 2193–2218, 2001.

- [BEN 04] BENZ U.C., HOFMAN P., WILLHAUCK G. *et al.*, “Multi-resolution, object-oriented fuzzy analysis of remote sensing data for GIS-ready information”, *ISPRS Journal of Photogrammetry and Remote Sensing*, vol. 58, no. 3, pp. 239–258, 2004.
- [BEN 14] BEN-DOR E., VARACALLI G., “SHALOM: space borne hyperspectral applicative land and ocean mission: a joint project of ASI-ISA an update for 2014”, *IGARSS’14*, Quebec, Canada, 2014.
- [BLA 06a] BLANSCHÉ A., WANIA A., GANÇARSKI P., “Comparison of MACLAW with several attribute selection methods for classification in hyperspectral images”, *ICDM Workshops 2006*, pp. 231–236. 2006.
- [BLA 06b] BLANSCHÉ A., GANÇARSKI P., KORCZAK J., “MACLAW: a modular approach for clustering with local attribute weighting”, *Pattern Recognition Letters*, vol. 27, no. 11, pp. 1299–1306, 2006.
- [BLA 10] BLASCHKE T., “Object-based image analysis for remote sensing”, *ISPRS Journal of Photogrammetry and Remote Sensing*, vol. 65, no. 1, pp. 2–16. 2010.
- [BON 06] BONAIUTO M., FORNARA F., BONNES M., “Indexes of perceived residential environment quality and neighbourhood attachment in urban environments: a confirmation study on the city of Rome”, *Landscape and Urban Planning*, vol. 65, no. 2003, pp. 41–52, 2006.
- [BON 15] BONAFONI S., ANNIBALLE R., PICHIERRI M., “Comparison between surface and canopy layer urban heat island using MODIS data”, *Joint Urban Remote Sensing Event (JURSE)*, Lausanne, Switzerland, pp. 1–4, 2015.
- [BOU 10] BOURGET E., LE DÛ-BLAYO L., “Cartographie des paysages : apport à l’analyse des trames vertes et bleues. Projets de paysage”, available at: http://www.projetsdepaysage.fr/fr/cartographie_des_paysages_apport_a_l_analyse_des_trames_vertes_et_bleue, 2010.
- [BRE 01] BREIMAN L., “Random forests”, *Machine Learning*, vol. 45, no. 1, pp. 5–32, 2001.
- [BRI 06] BRIOTTET X., LACHÉRADE S., PALLOTTA S. *et al.*, “Acquisition and analysis of a spectral and bidirectional database of urban materials over Toulouse (France)”, *SPIE Defense and Security Symposium, Targets and Backgrounds XII: Characterization and Representation Conference - SPIE 6239-29*, Orlando (Kissimmee), Florida, USA, 17–21 April 2006.
- [BRI 16] BRIOTTET X., “Radiometry in the optical domain”, in BAGHDADI N., ZRIBI M. (eds), *Optical Remote Sensing of Land Surfaces*, ISTE Press Ltd, London and Elsevier Ltd, Oxford, 2016.

- [BRU 05] BRÜCKER G., “Vulnerable populations: lessons learnt from the summer 2003 heat waves in Europe”, *EuroSurveillance*, vol. 10, no. 7, p. 551, 2005.
- [CAR 77] CARLSON T.N., AUGUSTINE J.A., BOLAND F.E., “Potential application of satellite temperature measurements in analysis of land use over urban areas”, *Bulletin of the American Meteorological Society*, vol. 58, pp. 1301–1303, 1977.
- [CAR 14] CARRÈRE V., BRIOTTET X., JACQUEMOUD S. *et al.*, “The French proposal for a high spatial resolution Hyperspectral mission”, EGU General Assembly, *Geophysical Research Abstracts*, EGU2014-11791, Vienna, Austria, vol. 16, 27 April–2 May 2014.
- [CAS 72] CASTELLS M., *La question urbaine*, François Maspero, Paris, p. 455, 1972.
- [CAV 08] CAVALLI R.M., FUSILLI L., PASCUCCI S. *et al.*, “Hyperspectral sensor data capability for retrieving complex urban land cover in comparison with multispectral data: Venice City case study (Italy)”, *Sensors*, vol. 8, pp. 3299–3320, 2008.
- [CHA 06] CHAMPION N., BOLDO D., “A robust algorithm for estimating digital terrain models from digital surface models in dense urban areas”, *International Archives of Photogrammetry, Remote Sensing and Spatial Information Sciences*, Bonn, Germany, vol. 36, no. 3, 2006.
- [CHE 11] CHEN M., PANG S., CHAM T. *et al.*, “Visual tracking with generative template model based on Riemannian manifold of covariances”, *Proceedings of 14th International Conference on Information Fusion (FUSION)*, pp. 1–8, 2011.
- [CHE 13] CHEN M., BRIOTTET X., PANG S.K., “Efficient empirical reflectance retrieval in urban environments”, *IEEE Journal of Selected Topics in Applied Earth Observations and Remote Sensing*, vol. 6, no. 3, pp. 1596–1602, 2013.
- [CLA 80] CLARCK J., The effect of resolution in simulated satellite imagery on spectral characteristics and computer assisted land use classification, report jet Propulsion Laboratory Report, pp. 75–22, 1980.
- [COM 02] COMANICIU D., MEER P., “Mean shift: a robust approach toward feature space analysis”, *IEEE Transactions on Pattern Analysis and Machine Intelligence*, vol. 24, no. 5, pp. 603–619, 2002.
- [DAL 05] DALAL N., TRIGGS B., “Histograms of oriented gradients for human detection”, *International Conference on Computer Vision and Pattern Recognition (CVPR’05)*, San Diego, United States, IEEE Computer Society, vol. 1, pp. 886–893, June 2005.

- [DAL 10] DALLA MURA M., BENEDIKTSSON J.A., WASKE B. *et al.*, “Morphological attribute profiles for the analysis of very high resolution images”, *IEEE Transactions on Geoscience and Remote Sensing*, vol. 48, no. 10, pp. 3747–3762, 2010.
- [DEL 08] DELM A.V., GULINCK H., “Classification and quantification of green in the expanding urban and semi-urban complex: application of detailed field data and IKONOS imagery”, *Ecological Indicators*, vol. 11, no. 1, pp. 52–60, 2008.
- [DIM 03] DIMOUDI, A., NIKOLOPOULOU M., “Vegetation in the urban environment: microclimatic analysis and benefits”, *Energy and Buildings*, vol. 35, no. 1, pp. 69–76, 2003.
- [DON 00] DONNAY J.P., COLLET C., WEBER C., *La télédétection en Francophonie: analyse critique et perspectives*, AUF, 2000.
- [DUP 12] DUPUY S., BARBE E., BALESTRAT M., “An object-based image analysis method for monitoring land conversion by artificial sprawl use of RapidEye and IRS data”, *Remote Sensing*, vol. 4, no. 2, pp. 402–423, 2012.
- [DUR 08] DURIEUX L., LAGABRIELLE E., NELSON A., “A method for monitoring building construction in urban sprawl areas using object-based analysis of Spot 5 images and existing GIS data”, *ISPRS Journal of Photogrammetry and Remote Sensing*, vol. 63, no. 4, pp. 399–408, 2008.
- [EP 05] Directive 2003/98/EC of the European Parliament and of the Council of 17 November 2003 on the re-use of public sector information (OJ L 345, 31.12.2003 p. 90), 2005.
- [FAU 14] FAUVEL M., PLANQUE C., SHEEREN D. *et al.*, “Télédétection des éléments semi-naturels: utilisation des données Pléiades pour la détection des haies”, *Revue Française de Photogrammétrie et de Télédétection*, vol. 208, pp. 111–116, 2014.
- [FLE 06] FLEYEH H., “Shadow and highlight invariant color segmentation algorithm for traffic signs”, *Proceedings of IEEE Conference on Cybernetics and Intelligent Systems*, Bangkok, Thailand, pp. 1–7, 7–9 June 2006.
- [GAN 08] GANÇARSKI P., BLANSCHÉ A., WANIA A., “Comparison between two coevolutionary feature weighting algorithms in clustering”, *Pattern Recognition*, vol. 41, no. 3, pp. 983–994, 2008.
- [GIL 98] GILLESPIE A., ROKUGAWA S., MATSUNAGA T. *et al.*, “A temperature and emissivity separation algorithm for Advanced Spaceborne Thermal Emission and Reflection Radiometer (ASTER) images”, *IEEE Transactions on Geoscience and Remote Sensing*, vol. 36, pp. 1113–1126, 1998.

- [GIV 98] GIVONI B., *Climate Considerations in Building and Urban Design*, John Wiley & Sons, New York, 1998.
- [GOE 85] GOETZ A.F.H., VANE G., SOLOMON J.E. *et al.*, “Imaging spectrometry for Earth remote sensing”, *Science*, vol. 228, no. 4704, pp. 1147–1153, 1985.
- [GOM 04] GÓMEZ F., GLI L., JABALOYES J., “Experimental investigation on the thermal comfort in the city: relationship with the green areas, interaction with the urban microclimate”, *Building and Environment*, vol. 39, pp. 1077–1086, 2004.
- [GRA 11] GRABER G., POCK T., BISCHOF H., “Online 3D reconstruction using convex optimization”, *ICCV Workshops*, pp. 708–711, 2011.
- [GRI 02] GRIGORESCU S.E., PETKOV N., KRUIZINGA P., “Comparison of texture features based on Gabor filters”, *IEEE Transactions on Image Processing*, vol. 11, no. 10, pp. 1160–1167, 2002.
- [GUI 06] GUIGUES L., COCQUEREZ J.P., LE MEN H., “Scale sets analysis”, *International Journal of Computer Vision*, vol. 68, no. 3, pp. 289–317, 2006.
- [GUL 05] GULYAS A., “Differences in human comfort conditions within a complex urban environment: a case study”, *Acta climatologica et chronologica, Universitatis Szegediensis*, vol. 38–39, pp. 71–84. 2005.
- [GUO 11] GUO L., CHEHATA N., MALLETT C. *et al.*, “Relevance of airborne LiDAR and multispectral image data for urban scene classification using Random Forests”, *ISPRS Journal of Photogrammetry and Remote Sensing*, vol. 66, no. 1, pp. 56–66, January 2011.
- [GUY 02] GUYON I., WESTON J., BARNHILL S. *et al.*, “Gene selection for cancer classification using support vector machines”, *Machine Learning*, vol. 46, pp. 289–422, 2002.
- [GUY 08] GUYADER A., “La biodiversité: un concept flou ou une réalité scientifique? ”, *Courrier de l’environnement de l’INRA*, no. 55, February 2008.
- [HAR 73] HARALICK R.M., SHANMUGAM K., DINSTEN I., “Textural features for image classification”, *IEEE Transactions on Systems, Man and Cybernetics*, vol. 3, no. 6, pp. 610–621, 1973.
- [HEI 12] HEINRICH V., KRAUSS G., GÖTZE C. *et al.*, “IDB – www.indexdata base.de, Entwicklung einer Datenbank für Fernerkundungsindizes”, *AK Fernerkundung*, vol. 10, pp. 4–5, 2012.
- [HER 04] HEROLD M., ROBERTS D.A., GERDNER M. *et al.*, “Spectrometry for urban area remote sensing—development and analysis of a spectral library from 350 to 2400 nm”, *Remote Sensing of Environment*, vol. 91, pp. 304–319, 2004.

- [HER 05] HEROLD M., ROBERTS D., “Spectral characteristics of asphalt road aging and deterioration: implication for remote sensing applications”, *Applied Optics*, vol. 44, no. 20, pp. 4327–4334, 2005.
- [HER 11] HEROLD M., SKUTSCH M., “Monitoring, reporting and verification for national REDD+ programmes: two proposals”, *Environmental Research Letters*, vol. 6, 2011.
- [HUB 12] HUBERT-MOY L., NABUCET J., VANNIER C. *et al.*, “Cartographie des continuités écologiques: quelles données pour quelles échelles territoriales? Application à la sous-trame forestière”, *Revue internationale de géomatique*, vol. 22, no. 4, pp. 619–640, 2012.
- [ING 07] INGLADA J., “Automatic recognition of man-made objects in high resolution optical remote sensing images by SVM classification of geometric image features”, *ISPRS Journal of Photogrammetry and Remote Sensing*, vol. 62, no. 3, pp. 236–248, 2007.
- [IOV 08] IOVAN C., BOLDO D., CORD M., “Detection, characterization and modeling vegetation in urban areas from high resolution aerial imagery”, *IEEE Journal of Selected Topics in Applied Earth Observations and Remote Sensing*, vol. 1, pp. 206–213, 2008.
- [JAT 08] JAT M.K., GARG P.K., KHARE D., “Modelling of urban growth using spatial analysis techniques: a case study of Ajmer city (India)”, *International Journal of Remote Sensing*, vol. 29, no. 2, pp. 543–567, 2008.
- [JEN 12] JENSEN R.R., HARDIN P.J., HARDIN A.J., “Classification of urban tree species using hyperspectral data”, *Geocarto International*, vol. 27, pp. 443–458, 2012.
- [JOH 04] JOHNSTON J., NEWTON J., *Building Green: a Guide to Using Plants on Roofs, Walls and Pavements*, Ecology Unit, London, 2004.
- [KAR 09] KARANTZALOS K., PARAGIOS N., “Recognition-driven two-dimensional competing priors toward automatic and accurate building detection”, *IEEE Transactions on Geoscience and Remote Sensing*, vol. 47, no. 1, pp. 133–144, 2009.
- [KAS 15] KASPERSEN P.S., FENSHOLT R., DREWS M., “Using Landsat vegetation indices to estimate impervious surface fractions for European cities”, *Remote Sensing*, vol. 7, pp. 8224–8249, 2015.
- [LAB 00] LABEN C., BROWER B., Process for enhancing the spatial resolution of multispectral imagery using pan-sharpening, U.S. Patent US 6 011 875, 2000.

- [LAC 08] LACHÉRADE S., MIESCH C., BOLDO D. *et al.*, “ICARE: a physically-based model to correct atmospheric and geometrical effects from high spatial and spectral remote sensing images over 3D urban areas”, *Meteorology and Atmospheric Physics*, vol. 102, no. 3, pp. 209–222, 2008.
- [LAG 04] LAGOUARDE J.P., MOREAU P., IRVINE M. *et al.*, “Airborne experimental measurements of the angular variations in surface temperature over urban areas: case study of Marseille (France)”, *Remote Sensing of Environment*, vol. 93, pp. 443–462, 2004.
- [LAN 09] LANDRY S.M., CHAKRABORTY J., “Street trees and equity: evaluation of the spatial distribution of an urban amenity”, *Environment and Planning*, vol. 41, pp. 2651–2670, 2009.
- [LEB 96] LEBLON B., GALLANT L., GRANBERG H., “Effects of shadowing types on ground-measured visible and near-infrared shadow reflectances”, *Remote Sensing of Environment*, vol. 58, no. 3, pp. 322–328, 1996.
- [LEB 11] LE BRIS A., CHEHATA N., “Change detection in a topographic building database using submetric satellite images”, *International Archives of Photogrammetry, Remote Sensing and Spatial Information Sciences (IAPRS)*, vol. 38, no. 3/W22, pp. 25–30, 2011.
- [LON 15] LONCAN L., ALMEIDA L.B., BIOCAS-DIAS J.M. *et al.*, “Hyperspectral pansharpening: a review”, *IEEE Geosci. and Remote Sens. Mag.*, 2015.
- [LU 06] LU D.S., WENG Q.H., “Use of impervious surface in urban land-use classification”, *Remote Sensing of Environment*, vol. 102, no. 1–2, pp. 146–160, 2006.
- [MAC 07] MACGRANAHAN G., “Urban environments, wealth and health: shifting burdens and possible responses in low and middle-income nations”, Human Settlements Working Paper, Urban Environments No. 1, International Institute for Environment and Development (IIED), London, UK, p. 53, 2007.
- [MAD 01] MADHAVAN B.B., KUBO S., KURISAKI N. *et al.*, “Appraising the anatomy and spatial growth of the Bangkok Metropolitan area using a vegetation-impervious soil model through remote sensing”, *International Journal of Remote Sensing*, vol. 22, no. 5, pp. 789–806, 2001.
- [MAI 12] MAIRE E., MARAIS-SICRE C., GUILLERME S. *et al.*, “High resolution remote sensing of trees and hedges using mathematical morphology”, *International Journal of Geomatics and Spatial Analysis*, vol. 22/4, pp. 519–538, 2012.

- [MAR 06] MARESCA B., RANVIER M., “Biodiversité : combien est-on prêt à payer ? Une méthode exploratoire appliquée au programme Natura 2000”, *Centre de Recherche pour l’Etude et l’Observation des Conditions de vie (CREDOC)*, vol. 198, p. 4, 2006.
- [MAR 15] MARMANIS D., DATCU M., ESCH T. *et al.*, “Deep learning Earth observation using ImageNet pretrained networks”, *IEEE Geoscience and Remote Sensing Letters*, vol. 13, no. 1, pp. 105–109, 2015.
- [MAT 06] MATHIEU N., “Pour un croisement transatlantique des recherches interdisciplinaires sur les socio-écosystèmes urbains”, *Natures Sciences Sociétés, NSS Dialogues*, EDP Sciences, vol. 14, pp. 15–18, 2006.
- [MAT 07] MATHIEU R., ARYAL J., CHONG A.K., “Object-based classification of Ikonos imagery for mapping large-scale vegetation communities in urban areas”, *Sensors*, vol. 7, no. 11, pp. 2860–2880, 2007.
- [MEA 05] MEA, Summary reports, available at: <http://www.millenniumassessment.org/fr/Synthesis.html>, 2005.
- [MNI 12] MNIH D., HINTON G.E., “Learning to label aerial images from noisy data”, *Proceedings of the 29th International Conference on Machine Learning (ICML-12)*, pp. 567–574, 2012.
- [MUR 13] MURATET A., LORILLIERE R., CLERGEAU P. *et al.*, “Evaluation of landscape connectivity at community level using satellite-derived NDVI”, *Landscape Ecology*, vol. 28, no. 1, pp. 95–105, 2013.
- [MYI 11] MYINT S.W., GOBER P., BRAZEL A. *et al.*, “Per-pixel vs. object based classification of urban land cover extraction using high spatial resolution imagery”, *Remote Sensing of Environment*, vol. 115, no. 5, pp. 1145–1161, 2011.
- [OKE 81] OKE T.R., “Canyon geometry and the nocturnal Urban Heat Island: comparison of scale model and field observations”, *Journal of Climatology*, vol. 1, pp. 237–254, 1981.
- [OKE 82] OKE T.R., “The energetic basis of the urban heat island”, *Quarterly Journal of the Royal Meteorological Society*, vol. 108, pp. 1–24, 1982.
- [OLT 10] OLTRA-CARRIÓ R. SOBRINO J.A. GUTIERREZ-ANGONESE J. *et al.*, “Estudio del crecimiento urbano, de la estructura de la vegetación y de la temperatura de la supereficie del Gran San Miguel de Tucumán, Argentina”, *Revista Nacional de Teledetección- Asociación Española de Teledetección*, vol. 34, pp. 69–76, 2010.
- [OLT 12] OLTRA-CARRIÓ R., SOBRINO J.A., FRANCH B. *et al.*, “Land surface emissivity retrieval from airborne sensor over urban areas”, *Remote Sensing of Environment*, vol. 123, pp. 298–305, 2012.

- [OLT 13] OLTRA-CARRIÓ R., Thermal remote sensing of urban areas. The case study of the Urban Heat Island of Madrid, PhD Thesis, University of València, Spain, 2013.
- [OLT 14] OLTRA-CARRIO R., CUBERO-CASTAN M., BRIOTTET X. *et al.*, “Analysis of the performance of the TES algorithm over urban areas”, *IEEE Transactions on Geoscience and Remote Sensing*, vol. 52, pp. 6989–6998, 2014.
- [PAI 15] PAISITKRIANGKRAI S., SHERRAH J., JANNEY P. *et al.*, “Effective semantic pixel labelling with convolutional networks and conditional random fields”, *Proceedings of the IEEE International Conference on Computer Vision and Pattern Recognition Workshops (CVPRW)*, pp. 36–43, 2015.
- [PAL 05] PAL M., MATHER P.M., “Support vector machines for classification in remote sensing”, *International Journal of Remote Sensing*, vol. 26, pp. 1007–1011, 2005.
- [PEU 95] PEUQUET D., DUAN N., “An event-based spatio-temporal data model (ESTDM) for temporal analysis of geographical data”, *International Journal of Geographical Information Systems*, vol. 9, no. 1, pp. 7–24. 1995.
- [PHA 11] PHAM H.M., YAMAGUCHI Y., BUI T.Q., “A case study on the relation between city planning and urban growth using remote sensing and spatial metrics”, *Landscape and Urban Planning*, vol. 100, no. 3, pp. 223–230, 2011.
- [PHA 12] PHAM T.T.H., APPARICIO P., SÉGUIN A.M. *et al.*, “Spatial distribution of vegetation in Montreal: an uneven distribution or environmental inequity?”, *Landscape and Urban Planning*, vol. 107, no. 3, pp. 214–224, 2012.
- [PIE 06] PIERROT-DESEILLIGNY M., PAPANODITIS N., “A multiresolution and optimization-based image matching approach: an application to surface reconstruction from SPOT5-HRS stereo imagery”, *IAPRS volXXXVI-1/W41 in ISPRS Workshop On Topographic Mapping From Space (With Special Emphasis on Small Satellites)*, Ankara, Turkey, 2006.
- [PLA 04] PLATT R.V., GOETZ A.F.H., “A comparison of AVIRIS and Landsat for land use classification at the urban fringe”, *Photogrammetric Engineering and Remote Sensing*, vol. 70, pp. 813–819, 2004.
- [POU 09] POULAIN V., INGLADA J., SPIGAI M. *et al.*, “Fusion of high resolution optical and SAR images with vector data bases for change detection”, *IEEE International Geoscience and Remote Sensing Symposium (IGARSS 09)*, Cape Town, South Africa, 2009.
- [PRE 08] PRÉVOT-JULLIARD A.C., SERVAIS V., “La ville, un dénominateur commun”, in *Entre l’Homme et la nature, une démarche pour des relations durables*, Unesco – notes techniques, Paris, pp. 86–87, 2008.

- [PUI 01] PUISSANT A., WEBER C., “Utilité des images haute résolution pour évaluer la place de la végétation dans l’aménagement urbain : Quelles résolutions pour quels besoins”, *V^{ème} rencontre Théo QUANT*, p. 10, 2001.
- [PUI 03] PUISSANT A., WEBER C., “Les images à très haute résolution spatiale : une source d’information géographique en milieu urbain? État des lieux et perspectives”, *L’Espace Géographique*, vol. 4, pp. 345–356, 2003.
- [PUI 04] PUISSANT A., HIRSCH J., “Télédétection urbaine et résolution spatiale optimale : intérêt pour les utilisateurs et aide pour les classifications”, *Revue Internationale de Géomatique*, vol. 14, no. 3–4, pp. 403–415, 2004.
- [PUI 14] PUISSANT A., ROUGIER S., STUMPF A., “Object-oriented mapping of urban trees using Random Forest classifiers”, *International Journal of Applied Earth Observation and Geoinformation*, vol. 26, pp. 235–245, 2014.
- [RAO 72] RAO P.K., “Remote sensing of urban heat islands from an environmental satellite”, *Bulletin of the American Meteorological Society*, vol. 53, pp. 647–648, 1972.
- [RAP 12] RAPINEL S., Contribution de la télédétection à l’évaluation des fonctions des zones humides: de l’observation à la modélisation prospective, thesis, University of Rennes 2, 2012.
- [RHE 14] RHEIN C., PALIBRK M., “Urban forms, land use and social mix in built up areas: the case of city of Paris”, *Topics Images & Villes, European Journal of Geography*, vol. 685, 27 July 2014.
- [RIC 03] RICHTER R., “Status of model ATCOR4 on atmospheric /topographic correction for airborne hyperspectral imagery”, *3rd EARSeL Workshop on Imaging Spectroscopy*, 13–16 May 2003.
- [RIG 06] RIGO G., PARLOW E., OESCH D., “Validation of satellite observed thermal emission with in-situ measurements over an urban surface”, *Remote Sensing of Environment*, vol. 104, pp. 201–210, 2006.
- [ROU 14] ROUGIER S., PUISSANT A., “Improvement of urban vegetation segmentation and classification using multi-temporal Pléiades images”, *Proceedings of the 5th Conference GEOBIA*, Thessaloniki, Greece, p. 409–414, 21–24 May 2014.
- [ROU 15] ROUSSET-ROUVIÈRE L., “Sysiphe system: a state of the art airborne hyperspectral imaging system: initial results from the first airborne campaign”, *EARSe*, Luxembourg, 14–16 April 2015.

- [ROT 07] ROTTENSTEINER F., “Building change detection from digital surface models and multi-spectral images”, *International Archives of the Photogrammetry, Remote Sensing and Spatial Information Sciences (IAPRS)*, vol. 36(3/W49B), Munich, Germany, 2007.
- [SAI 08] SAINT-GÉRARD T., “Understanding to measure... or measuring to understand”, in GUERMOND Y. (eds), *The Modeling Process in Geography*, ISTE, London and John Wiley & Sons, New York, 2008.
- [SEB 10] SEBARI I., MORIN D., “Développement et défis de la télédétection urbaine”, *Cahiers de géographie du Québec*, vol. 54, no. 151, pp. 117–132, 2010.
- [SCH 12] SCHINDLER K., “An overview and comparison of smooth labeling methods for land-cover classification”, *IEEE Transactions on Geoscience and Remote Sensing*, vol. 50, no. 11, pp. 4534–4545, 2012.
- [SHA 00] SHASHUA-BAR L., HOFFMAN M.E., “Vegetation as a climatic component in the design of an urban street: an empirical model for predicting the cooling effect of urban green areas with trees”, *Energy and Buildings*, vol. 31, no. 3, pp. 221–235, 2000.
- [SHI 11] SHIMONI M., TOLT G., PERNEEL C. *et al.*, “Detection of vehicles in shadow areas”, *Proceedings of 3rd Workshop on Hyperspectral Image and Signal Processing: Evolution in Remote Sensing, WHISPERS*, Lisbon, Portugal, pp. 1–4, 6–9 June 2011.
- [SID 14] SIDI YOUSSEF M.M., MALLET C., CHEHATA N. *et al.*, “Détection de bâtiments à partir d’une image satellitaire par combinaison d’approches ascendante et descendante”, *RFIA’14 (19^{ème} congrès national sur la Reconnaissance de Formes et l’Intelligence Artificielle)*, Rouen, France, June 2014.
- [SIM 15] SIMOES M., BIOCAS DIAS J., ALMEIDA L. *et al.*, “A convex formulation for hyperspectral image superresolution via subspace-based regularization”, *IEEE Trans. Geosci. and Remote Sens.*, 2015.
- [SMA 03] SMALL C., “High spatial resolution spectral mixture analysis of urban reflectance”, *Remote Sensing of Environment*, vol. 88, pp. 170–186, 2003.
- [SOB 08] SOBRINO J.A., JIMENEZ-MUNOZ J.C., SORIA G. *et al.*, “Land surface emissivity retrieval from different VNIR and TIR sensors”, *IEEE Transactions on Geoscience and Remote Sensing*, vol. 46, pp. 316–327, 2008.

- [SOB 12a] SOBRINO J.A., OLTRA-CARRIÓ R., JIMÉNEZ-MUÑOZ J.C. *et al.*, “Emissivity mapping over urban areas using a classification-based approach: application to the Dual-use European Security IR Experiment (DESIREX)”, *International Journal of Applied Earth Observation and Geoinformation*, vol. 18, pp. 141–147, 2012.
- [SOB 12b] SOBRINO J.A., OLTRA-CARRIÓ R., SÒRIA G. *et al.*, “Impact of spatial resolution and satellite overpass time on evaluation of the surface urban heat island effects”, *Remote Sensing of Environment*, vol. 117, pp. 50–56. 2012.
- [SOB 13] SOBRINO J.A., OLTRA-CARRIÓ R., SÒRIA G. *et al.*, “Evaluation of the surface urban heat island effect in the city of Madrid by thermal remote sensing”, *International Journal of Remote Sensing*, vol. 34, pp. 3177–3192, 2013.
- [STA 07] STATHOPOULOU M., CARTALIS C., PETRAKIS M., “Integrating Corine Land Cover data and Landsat TM for surface emissivity definition: application to the urban area of Athens, Greece”, *International Journal of Remote Sensing*, vol. 28, pp. 3291–3304, 2007.
- [STA 09] STATHOPOULOU M., SYNNEFA A., CARTALIS C. *et al.*, “A surface heat island study of Athens using high-resolution satellite imagery and measurements of the optical and thermal properties of commonly used building and paving materials”, *International Journal of Sustainable Energy*, vol. 28, pp. 59–76, 2009.
- [STE 06] STEWART I.D., OKE T.R., “Methodological concerns surrounding the classification of urban and rural climate stations to define urban heat island magnitude”, Preprints, *6th International Conference on Urban Climate*, Goteborg, Sweden, 12–16 June 2006.
- [SU 11] SU S., JIANG Z., ZHANG Q. *et al.*, “Transformation of agricultural landscapes under rapid urbanization: a threat to sustainability in Hang-Jia-Hu region, China”, *Applied Geography*, vol. 31, pp. 439–449, 2011.
- [STU 90] STULPNAGEL A. VON, HORBERT M., SUKOPP H., “The importance of vegetation for the urban climate”, in SUKOPP H., HEJNY S., KOWARIK I. (eds), *Urban Ecology*, SPB Academic Publishing, The Hague, 1990.
- [TIA 08] TIANGCO M., LAGMAY A.M.F., ARGETE J., “ASTER based study of the night time urban heat island effect in Metro Manila”, *International Journal of Remote Sensing*, vol. 29, pp. 2799–2818, 2008.
- [TOM 98] TOMASI C., ANDUCHI R.M., “Bilateral filtering for gray and color images”, *Proceedings of IEEE International Conference on Computer Vision*, pp. 836–846, 1998.

- [VAN 93] VANDEGRIEND A.A., OWE M., “On the relationship between thermal emissivity and the normalized difference vegetation index for natural surfaces”, *International Journal of Remote Sensing*, vol. 14, pp. 1119–1131, 1993.
- [VAN 03] VAN HERZELE A., WIEDEMANN T., “A monitoring tool for the provision of accessible and attractive urban green spaces”, *Landsc. Urban Plan.*, vol. 966, pp. 1–18, 2003.
- [VAN 11] VANNIER C., HUBERT-MOY L., NABUCET J., “Analyse spatiale de la dynamique de l’occupation du sol aux échelles de la parcelle et de l’îlot parcellaire, application en paysage bocager”, *Revue Internationale de Géomatique*, vol. 21, no. 3, pp. 353–374, 2011.
- [VOO 02] VOOGT J.A., “Urban Heat Island”, in MUNN T. (ed.), *Encyclopedia of Global Environmental Change*, Wiley, Chichester, 2002.
- [VOO 03] VOOGT J.A., OKE T.R., “Thermal remote sensing of urban climates”, *Remote Sensing of Environment*, vol. 86, pp. 370–384, 2003.
- [WAN 07a] WANIA A., WEBER C., “Hyperspectral imagery and urban green observation”, *Proceedings of Urban Remote Sensing Joint Event*, pp. 1–8, 11–13 April 2007.
- [WAN 07b] WANIA A., Urban vegetation: detection and function evaluation for air quality assessment, PhD thesis, University Louis Pasteur, 2007.
- [WEB 15] WEBER C., “Formes urbaines et facteurs environnementaux: exposition et santé urbaine”, *Environment, Risques & Santé*, vol. 14, no. 4, pp. 305–312, 2015.
- [WEI 15] WEI Q., BIUCAS DIAS J.M., DOBIGEON N. *et al.*, “Hyperspectral and multispectral image fusion based on a sparse representation”, *IEEE Trans. Geosci. and Remote Sens.*, vol. 53, no. 7, pp. 3658–3668, 2015.
- [WEL 82] WELCH R., “Spatial resolution requirements for urban studies”, *International Journal of Remote Sensing*, vol. 3, no. 2, pp. 139–146, 1982.
- [WEN 07] WENG Q., QUATTROCCHI D.A., *Urban Remote Sensing*, CRC Press, 2007.
- [WEN 12] WENG Q., “Remote sensing of impervious surfaces in the urban areas: requirements, methods, and trends”, *Remote Sensing of Environment*, vol. 117, 2012.
- [WGI 14] WGIIARS, Intergovernmental panel on climate change, “Working Group II Contribution to the 5th assessment report of the intergovernmental panel on climate change”, *Urban Areas*, 2014.

- [WIL 11] WILSON E., TERMEER C., MEES H.P. *et al.*, “Adaptation to climate change in urban areas: climate-greening London, Rotterdam, and Toronto”, *Climate Law*, vol. 2, no. 2, pp. 251–280, 2011.
- [WU 03] WU C., MURRAY A.T., “Estimating impervious surface distribution by spectral mixture analysis”, *Remote Sens. Environ.*, vol. 84, pp. 493–505, 2003.
- [YOK 12] YOKOYA N., YAIRI T., IWASAKI A., “Coupled nonnegative matrix factorization unmixing for hyperspectral and multispectral data fusion”, *IEEE Trans. Geosci. and Remote Sens.*, vol. 50, no. 2, pp. 528–537, 2012.
- [ZHA 09] ZHANG X., ZHONG T., FENG X. *et al.*, “Estimation of the relationship between vegetation patches and urban land surface temperature with remote sensing”, *International Journal of Remote Sensing*, vol. 30, no. 8, pp. 2105–2118, 2009.
- [ZHA 10] ZHANG X., FENG X., JIANG H., “Object-oriented method for urban vegetation mapping using IKONOS imagery”, *International Journal of Remote Sensing*, vol. 31, no. 1, pp. 177–196, 2010.
- [ZHO 08] ZHOU W., TROY A., “An object-oriented approach for analysing and characterizing urban landscape at the parcel level”, *International Journal of Remote Sensing*, vol. 11, no. 10, pp. 3119–3135, 2008.
- [ZIN 15] ZINKO S., “Traitement de Données Hyperspectrales”, Master Observation de la Terre et Géomatique, University of Strasbourg, p. 30, 2015.